Composite Structures 227 (2019) 111244

Contents lists available at ScienceDirect

Composite Structures

journal homepage: www.elsevier.com/locate/compstruct

Carbon nanotube (CNT) incorporated cementitious composites for functional construction materials: The state of the art

G.M. Kim[a], I.W. Nam[b], Beomjoo Yang[c], H.N. Yoon[d], H.K. Lee[d,*], Solmoi Park[d,e]

[a] Korea Institute of Geoscience and Mineral Resources, 124 Gwahak-ro, Yuseong-gu, Daejeon 34132, Republic of Korea
[b] College of Civil Engineering, Nanjing Tech University, 30 Puzhu Road(S), Nanjing, Jiangsu Province 211800, China
[c] School of Civil Engineering, Chungbuk National University, 1 Chungdae-ro, Seowon-gu, Cheongju, Chungbuk 28644, Republic of Korea
[d] Department of Civil and Environmental Engineering, Korea Advanced Institute of Science and Technology (KAIST), 291 Daehak-ro, Yuseong-gu, Daejeon 34141, Republic of Korea
[e] Applied Science Research Institute, Korea Advanced Institute of Science and Technology (KAIST), 291 Daehak-ro, Yuseong-gu, Daejeon 34141, Republic of Korea

ARTICLE INFO

Keywords:
Carbon nanotube
Cementitious composites
Functionality
Dispersion
Application

ABSTRACT

Carbon nanotube (CNT) is one of the most promising nanomaterials, which has remarkable mechanical, electrical, thermal properties and chemical stability. Since the incorporation of CNT may dramatically improve the mechanical, electrical, thermal properties of composites, numerous studies on the fabrication and characterization of cementitious composites with CNT have been extensively conducted by researchers. Especially, the studies on the development of functional cementitious composites utilizing CNT have attracted much attention in the construction field. This paper introduces the state of art studies on the fabrication technologies of CNT-incorporated cementitious composites and provides in-depth information on the functional characteristics of the composites. Specifically, various dispersion techniques of CNT particles in cementitious materials are revisited to conclude on the pros and cons of those techniques. Furthermore, the mechanical properties, electromagnetic shielding and sensing performances, and heat generation characteristics of cementitious composites with CNT are extensively reviewed.

1. Introduction

Since the discovery of carbon nanotube (CNT) by Iijima in 1991 [1], a vast number of studies was conducted to verify its remarkable mechanical, thermal, electrical and chemical properties [2–7]. These outstanding properties are reported to be particularly useful for the application as reinforcement for composite materials, field emission sources, molecular sensors, super-capacitors and hydrogen containers [8–11].

Manufacture of CNT-incorporated composite materials is also an area of intensive research, since CNT provides ideal and desirable properties as a filler in composites in terms of mechanical, thermal, and electrical characteristics [12–15]. The major issue on the fabrication of composites incorporating CNT is to ensure proper dispersion of CNT particles in composites. Carbon nanotubes can be readily agglomerated by the strong attraction forces, thereby leading to the deterioration of the mechanical, electrical and thermal properties of the composites with CNT [16]. Thus, various techniques to properly disperse CNT in composites were attempted, and studies on the evaluation of dispersion state of CNT were simultaneously conducted [16–28].

The incorporation of CNT into polymer-based composites was initiated in late 1990s [12,29,30] with focuses on improving the mechanical, electrical and thermal properties of the composites [31,32]. The incorporation of CNT in cementitious binder was first introduced in early 2000s as means of developing functional cementitious composites applicable for construction fields [33], and nowadays, the practical applications of these composites have been provided, i.e., electromagnetic interference shielding material [34], piezoresistive/damage sensor [20], heating composite [16], and high strength cementitious material [35].

The present paper provides in-depth information on the structure and the extraordinary properties of CNT, revisits various dispersion techniques of CNT applied to the fabrication of cementitious composites from the mechanistic viewpoint, and introduces a number of methods that can effectively evaluate and predict the dispersion state of CNT in cementitious composites. Existing literatures regarding cementitious composites incorporating CNT mostly concern their mechanical properties and piezoresistive characteristics [36–41], while this paper

* Corresponding author.
E-mail address: haengki@kaist.ac.kr (H.K. Lee).

https://doi.org/10.1016/j.compstruct.2019.111244
Received 10 February 2019; Received in revised form 18 July 2019; Accepted 26 July 2019
Available online 27 July 2019

systematically revisits studies on heating and electromagnetic wave shielding characteristics of cementitious composites incorporating CNT, and modelling approaches for prediction of properties of these composites to discuss their use as a functional construction material.

2. Carbon nanotube

2.1. Structure and properties of CNT

(a) Structural characteristics: Carbon nanotube is placed between fullerenes and graphite, which is seemingly slender fullerenes. The walls of CNT is graphite-like structure and each end consists of a cap with half of a fullerene molecule [3]. Carbon nanotubes can be categorized by two main types, a single walled nanotube (SWNT) and a multi-walled nanotube (MWNT). The former consists of one layer of seamless single graphite sheet with a diameter of 1.0–2.0 nm [42]. The latter consists of layers of SWNTs and has a diameter of 2.0–100 nm [42].

Each C atom in atomic scale in CNT is aligned at 120° in the xy plane, composing hexagonal lattice [43]. The sp^2 hybridization composes 3-coordinates in local C environment with C–C bond length of 1.42 Å [44], thereby provides even interatomic alignment [43], though the presence of weak π bond persists in the z plane perpendicular to the xy plane. The Pz orbital induces van der Wall interactions and is responsible for the remarkable electrical conductivity of CNT [45].

The electrical characteristic may vary with the chirality of CNT, despite the identical intramolecular chemical bonding. Depending on the chirality, CNT can be classified as armchair, zigzag and chiral [45]. The chirality is determined by the orientation of the two dimensional graphene sheet, and can be defined in terms of the unit cell and using the chiral vector, as defined in Eq. (1) [45]

$$C_n = ma_1 + na_2 \quad (1)$$

where, a_1 and a_2 are unit vector in the two dimensional hexagonal lattice, and n and m are integers. m and n are used to compute the chiral angle in Eq. (2) [45]

$$\theta = \tan^{-1}(\sqrt{3}m/(2n + M)),\ 0 \le |\theta| \le \pi/6 \quad (2)$$

The chiral angle of CNT with an armchair type is π/6, meaning that its C–C bond is perpendicular to the tube axis, and therefore this type of CNT exhibits a metallic behavior [46]. The chiral angle of a zigzag type is zero, meaning that its C–C bond is parallel to the tube axis, and it behaves quasi-metallic [46]. CNT with other angle is referred to as chiral type [46].

(b) Mechanical properties: CNT was expected to exhibit exceptionally high mechanical properties, owing to its C–C bond which resembles that of graphite and is one of the strongest bond naturally abundant [47]. Graphite, for instance, has a modulus of 1.06 TPa and tensile strength of 130 GPa owing to the C–C bond [48]. The mechanical properties of CNT were initially measured by means of computational simulations, which calculated the young's modulus of short SWNT from theoretical basis and estimated as 1.5 TPa [49].

The Young's modulus of individual MWNT was first mechanically measured by [50] using the amplitude of intrinsic thermal vibration observed using TEM [50]. In the study, the average young's modulus of MWNT was reported to be 1.0–1.8 TPa [50]. Wong et al. [51], who took the first direct measurement of mechanical properties of MWNT by measuring the stiffness contact of arc-MWNT pinned at one end using atomic force microscope (AFM), reported that the average young's modulus was 1.28 TPa [51]. Other studies, in which the bending force of individual MWNT was measured inside the AFM, showed Young's modulus of MWNT in a range of 0.32–1.47 TPa [52–56].

(c) Electrical properties: the exceptional electrical properties of CNT are attributed to its one-dimensional characteristic and peculiar electronic structure of graphite [57]. In particular, the one-dimensional characteristic of CNT is closely related to the quantum confinement of electrons normal to the tube axis [45]. The electrons in the radial direction are restrained by the graphene sheet. Under this restraint, the electrons are bound to only propagate along the tube axis [45], meaning that the electrons inside the tube do not easily scatter, which is responsible for its extremely low electrical resistivity. Another factor attributable for its low electrical resistivity is its current density, which is highest of any known material (10^9 A/cm^2) [58,59].

The first transport measurement on bundles of MWNTs was conducted by [60] in 1994 using two gold contacts (also known as lithographic technique) and reported the electrical resistivity of MWNTs bundles of $\approx 10^{-3}$ Ω·cm [60]. The authors also reported the temperature-dependency of its resistance, which well-fitted a simple two-band semi-metal model between 2.0 and 300 K. Later on, the resistivity of individual MWNT was measured at an ambient temperature and was reported to be approximately 5.1×10^{-6}–1.2×10^{-4} Ω·cm [61,62].

(d) Thermal properties: it is presumable that the thermal conductivity of CNT along the tube axis is exceptionally high and possibly highest among all existing materials [63]. Phonon conduction mechanism is known to govern the thermal conductivity of CNT, similar with other non-metallic material [64], and is influenced by several factors such as various phonon active modes, the boundary surface scattering, the length of the free path for the phonons [65,66]. The phonon conduction in CNT is also largely affected by the atomic arrangement, its diameter and length, the presence of structural defects and impurities, and its morphology [67–69]. The direct and quantitative measurement of thermal conductivity of individual CNT is extremely difficult, and thus, most studies have been based on the theoretical simulations and indirect experimental tools. These results do show a significant scattered range of 2000–6000 W/mK [70–72].

Meanwhile, there were attempts of directly measuring the thermal conductivity of CNT in the past [64,73]. The thermal conductivity of an individual SWNT measured using a suspended micro-device was reported to be more than 2000 W/mK, and showed a decrease with a decrease in the temperature [73]. Moreover, the thermal conductivity of a MWNT measured using a micro-fabricated suspended device at an ambient temperature was more than 3000 W/mK [74]. These values were in the range of the results obtained by theoretical simulations and even showed less scatter for some instances, but more validations by direct measurement should be provided.

2.2. Agglomeration effect

Due to the exceptional mechanical, electrical and thermal properties of CNT, there have been an enormous number of studies with a focus on fabricating CNT-incorporated composites [75–77]. Nevertheless, these studies often reported the performance of the CNT-incorporated composites exhibiting far less than that theoretically expected [75–77]. This phenomenon is attributed to the agglomeration effect of CNT particles, which arises from its high aspect ratio and flexibility, tubular shape, and van der Waals interaction [78,79]. The high specific surface area of CNT inevitably increases its van der Waals force, meaning that it causes CNT particles to remain agglomerated. The attraction energy between tubes is reported to be 500 eV/μm [80]. The agglomeration effect of CNT causes discontinuity among tubes, leading to a substantial decline in the electrical and thermal performance of CNT-incorporated cementitious composites [81]. Moreover, Vaisman et al. [82] reported that a crack in CNT-incorporated cementitious composites was initiated from CNT particles that are agglomerated [82], suggesting that CNT agglomeration may weaken the overall mechanical performance of the composites.

3. Dispersion techniques

3.1. Ultrasonication

Ultrasonication is one of techniques commonly used for dispersion

of CNT particles in fluid medium [83], which converts line voltage into mechanical vibrations. The converted mechanical vibrations are then transferred into the fluid from the probe creating pressure waves, which increases the temperature of the fluid by cavitation [84]. The ultrasonication of CNT induces high local shear, particularly on the tube end, creating spaces among the particles [82,85], and therefore has been an effective means of dispersing CNT particles in liquid media with a low viscosity, i.e., water, acetone and ethanol [86]. For the fabrication of cementitious composites incorporating CNT, the suspension, in which CNT particles are uniformly dispersed via ultrasonication, has been used to produce cementitious materials [85,87]. Konsta-Gdoutos et al. [85] conducted a study on the dispersion of CNT in cementitious composites by a combination of ultrasonication and surfactants, and reported that at least 70 Pa of ultrasonic energy was needed [85]. Nevertheless, aggressive and long duration of ultrasonication treatment was reported to easily damage CNT, and this can be worsened by using a probe sonicator [88]. Particularly, the graphene structures of CNT can be utterly destroyed, inducing the conversion of tube structures into amorphous nanofibers in extreme cases [89]. Consequently, the localized damage in CNT adversely affects the electrical and mechanical properties of CNT-incorporated cementitious composites [86]. Moreover, entrapped pores can be formed in cementitious composites by the sonication process, thereby reducing the overall mechanical properties of the composites [90].

3.2. Admixtures

Various types of surfactants thus far have been successfully used as an agent for dispersing CNT particles in polymer composites [82,91]. Anionic sodium dodecyl sulfate (SDS) is a typical surfactant commonly used to achieve such purposes, while its use as a dispersion agent in cementitious composites poses a question [92]. Yazdanbakhsh et al. [93] reported that the use of the surfactants often used in polymer composites inhibited the hydration of cement, thereby weakens the mechanical properties of the composites [93]. In addition, despite that a satisfactory degree of dispersion of CNT in an aqueous medium can be achieved by using the surfactants, the CNT particles uniformly dispersed in the suspension can re-agglomerate when the suspension is mixed with cementitious materials [93]. Therefore, numerous studies were thereafter pioneered to explore the effect of commonly used cement admixtures on the dispersion of CNT in cementitious composites. Collins et al. [94] investigated the effect of typical cement admixtures such as air entrainer, styrene butadiene rubber, polycarboxylate-type superplasticizer on the dispersion of CNT in cementitious composites [94]. In the previous study, polycarboxylate-type superplasticizer was found to be the most effective dispersion agent, owing to its long lateral ether chains which induce steric repulsion [94]. Other types of superplasticizers such as nonionic polyoxythylene(23) laurylether [92], the mixture of sodium dodecyl benzene sulfonate (SDBS) and Triton X-100 (TX10) [95], methylcellulose [96], pluronic F-127 [97] were also found to be adequate for dispersion of CNT particles without causing adverse effects on the hydration of cement.

3.3. Silica fume

Silica fume can be used to disperse CNT in cementitious composites. Numerous studies reported the use of silica fume as a dispersion agent for fillers such as carbon fiber, prior to being considered as a dispersion agent for CNT [98,99,212]. Their spherical-shaped particles effectively infiltrates and increases the distance between the fillers incorporated in cementitious composites [98,99]. Recently, silica fume is widely used to serve this purpose, uniformly dispersing CNT in cementitious composites [16,90,100]. Kim et al. [90] conducted an SEM analysis on the CNT-incorporated cementitious composites using silica fume as a dispersion agent, and showed that the silica fume remained its spherical shape and infiltrated between CNT agglomerates, thereby reducing the size of CNT agglomerates [90]. The pozzolanic reaction of silica fume incorporated in cement begins at 3–7 days age [16]. That is, the spherical shape of silica fume was preserved during the mixing and casting, thereby physically contributing the dispersion of CNT through ball-bearing effect [90].

Nevertheless, silica fume alone may not be sufficient to disperse CNT particles; for instance, Kim et al. [101] reported that the dispersion of CNT in cementitious composites is only slightly improved by the sole use of silica fume, while it is vastly improved by simultaneous use of polycarboxylate-type superplasticizer [101]. It is presumed from the findings that the use of superplasticizers can create the gap needed for the infiltration of silica fume, thereby further enhances the dispersion of CNT [101].

3.4. Minimization of water-to-binder ratio

A water-to-binder (w/b) ratio is an important factor which influences the dispersion degree of CNT particles in cementitious composites. Kim et al. [100] experimentally showed that the electrical performance and its stability were improved by lowering the w/b ratio [100], meaning that the continuity of CNT network was improved as lowering w/b ratio. The w/b ratio of cementitious composites is closely related to their pore structure. An increase in w/b ratio is generally accepted to increase the porosity of cementitious composites [102], which can adversely influence the dispersion of CNT. The formation of pores with diameters greater than 1.0 μm induces the agglomeration of CNT particles (as found with the case when the CNTs have diameters of 10–40 nm and lengths of few μm). Nochaiya and Chaipanich [103] reported that the incorporation of CNT in cementitious composites reduced the amount of mesopores [103]. That is, pores with a large diameters are formed in cementitious composites at high w/b ratio and CNT particles incorporated in the pore solution remain poorly dispersed as the water is evaporated from these pores [16,100,104]. In contrast, the cementitious composites with a lower w/b ratio inherits much less amount of large pores, in which the agglomeration of CNT in the pore solution is minimized [100,103].

3.5. Modification of CNT

Various techniques for the surface modification of CNT have been suggested in order to enhance the dispersion of CNT; creating polar impurities such as OH or COOH end groups, decoration with polymer, CNT wrapping with non-linear polymers, and growing polymer chains on the surface and annealing of CNT [105–109]. Acid treatment has been the most widely used technique which creates functional groups on the surface of CNT for the use in the fabrication of CNT-incorporated cementitious composites [96,110–112]. Li et al. [96] used H_2SO_4 and HNO_3 to modify CNT, and formed carboxylic acid groups on the surface of CNT with higher dispersion characteristics in cementitious composites [96]. The functional groups on the surface of CNT reduces the contact angle and increases the wettability of CNT in contact with water, thereby enhances the dispersion of CNT [110]. Cwiren et al. [110] reported that the CNT functionalized with polyacrylic polymer in an aqueous solution remained well-dispersed over a period of 2 months [110]. Nevertheless, the dispersion characteristic of functionalized CNT is significantly affected by the presence of Ca^{2+} ions, that is, the functional groups on the surface of CNT can react with these ions, causing re-agglomeration of CNT in cementitious composites. In a study conducted by [111], it showed that few walled CNT (FWNT) functionalized with H_2SO_4 and HNO_3 underwent a chemical reaction with Ca^{2+}, and CNT particles were agglomerated [111].

Annealing treatment of CNT is occasionally reported in the previous study for enhancing the dispersion of CNT in cementitious composites [109]. Despite that the chemical vapor deposition (CVD) technique can be used for large scale production of CNT at a relatively low cost [109], the individual CNT produced by this technique often suffers from

defects along the graphene walls, and are curved, thus have lower strength and are difficult to be dispersed [75]. The annealing treatment of CNT can reduce the degree of lattice defects in the walls of CNT, effectively straightening the tubes, reducing the likelihood of agglomeration, thereby improving the dispersion of CNT [109].

4. Evaluation of dispersion state

Evaluating the dispersion state of CNT in cementitious composites is as important as ensuring the dispersion. Generally, techniques employed for evaluation of the dispersion can be broadly divided into those based on 1) image analysis and 2) resistivity measurement.

The image analysis technique utilizes SEM, AFM, and optical microscope to assess the degree of CNT agglomeration, in relation to cement hydrates from the obtained images. SEM image analysis is most widely used for evaluating the dispersion state of CNT, as reported in previous studies [85,90,96]. The dispersion state of CNT in cementitious composites can be directly observed via this technique. Kim et al [90] applied the SEM image analysis and observed the relative reduction of CNT agglomerates in cementitious composites when using silica fume as a dispersion agent [90]. Sanchez and Ince [113] also conducted a SEM image analysis on a CNT-incorporated cementitious composite, particularly focusing on the pocket of CNT agglomerates, thereby assessing the distribution state and the size of agglomeration [113]. Nochaiya and Chaipanich [103] adopted energy dispersive spectroscopy (EDS) and conducted carbon element mapping to evaluate the dispersion state of CNT [103]. Use of AFM is occasionally adopted to evaluate the dispersion state of CNT. Singh et al. [114] conducted AFM analysis on the surface of a CNT-incorporated cementitious composite, and assessed the roughness and the height variation of the CNT particles, thereby indirectly evaluating the dispersion state [114]. In addition, an optical microscope with a low magnification was adopted to evaluate the dispersion state of CNT incorporated in white cement binder [115]. Overall, image-based analyses qualitatively evaluate the dispersion state of CNT.

Another technique for evaluating dispersion state of CNT in cementitious composites is the measurement of DC electrical resistivity [16,100,104,114–117]. A lower electrical resistivity of CNT-incorporated cementitious composite indicates that the electrically conductive pathway in the composites is well formed by the proper dispersion of CNT [90]. Electrodes such as a metal plate should be embedded to measure the electrical resistivity of the CNT-incorporated cementitious composite [100]. In general, copper plates are widely used for this purpose [100]. The electrodes are covered by silver pastes to minimize the contact resistance between electrodes and the composite [100]. The methods for the measurement of DC electrical resistivity are categorized by the number of electrodes; two probe method with two electrodes and four probe method with four electrodes [118]. The major difference between the two methods is that the resistance of electrodes and the resistance between electrodes and the composite can be negligible in the four probe method [118]. Thus, the electrical resistivity measured by four probe method is generally lower than that measured by the two probe method [118].

Meanwhile, the measurement of DC electrical resistivity can be used to evaluate the continuity of electrically conductive pathway formed by CNT particles [16]. Some ions dissolved from cement particles remain in the pore solution of the composite, leading polarization effect [119]. A polarization effect is caused by the accumulation of electrical charges nearby electrodes which show opposite polarity to the charges, leading an increase in the electrical resistivity of the CNT-incorporated cementitious composite over time [120]. The effect of polarization become possibly significant when the electrically conductive pathways formed in the composite is inhomogeneous [16]. That is, the measurement of DC electrical resistivity of CNT-incorporated cementitious composite can be applied to evaluate the continuity of electrically conductive pathways in the CNT-incorporated cementitious composite [16].

Conduction of electricity through a CNT-incorporated cementitious composite mainly occurs via ionic conduction and electronic conduction [121]. Firstly, ionic conduction is induced by the presence of ionic components such as Ca, Mg, Al and Si, meaning that the presence of these components in the pore solution naturally induces the ionic conduction [122]. Note that the electrical resistivity of the pore solution in cementitious composites is approximately 250–350 Ω·cm [123]. Specifically, the ionic conduction has significant effect on the resistivity of composites with poor dispersion of CNT [124]. That is, the resistivity of the composites varies significantly depending on the amount of pore solution.

On the other hand, the electronic conduction of CNT is determined by the electrically conductive network formed by CNT particles in the composites. For instance, cementitious composites with well-distributed CNT possesses homogeneous conductive network, which induces electronic conduction. There exists a threshold, in which a certain amount of conductive filler incorporated in the composite improves the continuity of the network among the fillers, thereby significantly reduces the resistivity of the composite, and it is generally referred to as a percolation phenomenon [125]. The resistivity of such a composite is unaffected by the further incorporation of conductive fillers, once its percolation threshold is reached [125]. Therefore, it is mandatory to dry the samples to minimize the effect of ionic conduction before measuring the resistivity of CNT-incorporated cementitious composites [16,90,100].

The relationship between the dispersion techniques and DC resistivity of a composite reported in previous studies [16–28,100] is summarized in Fig. 1. It is suggested that the minimization of w/b, and use of surfactant and silica fume were found to be the most effective dispersion technique, as well as the use of surfactant and sonication. This is due to that physicochemical means of dispersing CNT in cementitious composites via multiple techniques is superior over dispersion via sole mechanism.

5. Theoretical analysis and prediction on CNT-incorporated cement composite properties

5.1. Recent advances in modeling of cement and cement-based nanocomposite

The rapid advances in computational power have facilitated the theoretical prediction of cementitious materials [126]. In the early years, the atomistic scale simulations considering the size of CNT particle have provided perspectives in cement science [127] and have important implications with regard to the cement-based nanocomposites [76]. The atomistic approaches such as the ab initio [128,129], the molecular dynamics (MD) [130–133], and the energy minimization

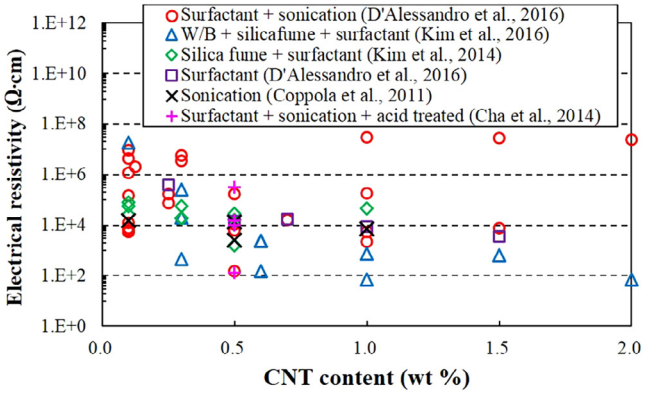

Fig. 1. Relationship between the dispersion techniques and DC resistivity measurement for cementitious composites with CNT [11–15,17–23,96].

technique [134,135], have extended the knowledge of the complex cementitious system, and demonstrated its effectiveness for understanding the material properties at the nanoscale [136–138].

The atomistic modeling is, however, inaccessible to such CNT-incorporated cementitious composites due to its inherent size limitation. Based on the calculation by [139], the spacing between adjacent CNT particles (diameter of 10 nm and length of 1 μm) incorporated in a cement paste with w/b of 0.35 and CNT amount of 0.5 wt% is approximately 440 nm [139]. Provided that the analysis range of the atomistic simulation is still several nanometers [140], the CNT/cement phase is difficult to generalize as a representative volume element (RVE) for the atomistic modeling.

In addition, cement materials still remain the basic questions and controversy regarding the chemical structure and composition [141]. The theoretical study on the cement itself and the nano-inclusions incorporated cementitious composites is thus expected to be performed in parallel in the future [142]. A multi-scale modeling has been developed in the various material schemes, while not been actively applied for the cementitious composite science owing to the above-mentioned reasons. To date, the alternative approaches with few assumptions, including the continuum model and/or numerical computation have been applied for the prediction of the CNT particles on the mechanical, electrical and dispersion properties of the cementitious composites [143].

5.2. Theoretical methods for CNT-incorporated cementitious composites

In the classical composites theory, the upper-bound value for the Young's modulus of CNT-reinforced cement based materials can be predicted by the following expression [144]:

$$E_c = V_m E_m + V_f E_f \tag{3}$$

where E and V signify the Young's modulus and the volume fraction, and the subscript c, m and f represent the composite, matrix, and filler, respectively. Within the formalism, the composite material is assumed to follow the parallel spring model, and the two phases of the composite are subject to uniform strain [144,145]. The classical composite theory can be used to serve as a reference. However, the classical theory is known to be not suitable for a precise prediction of CNT-incorporated cementitious composites, because it is not developed for nanocomposite, especially ignoring the size, shape, and chemophysical characteristics of CNT [146].

Hence, the continuum model based on the classical composite theory and Eshelby's equivalent inclusion method [147,148] has been introduced to improve the calculation precisions of CNT-incorporated cementitious composites by taking into account the interfacial and morphological effects [149]. According to [150] and [151], a self-consistent effective-medium formulation is proposed to predict the effective electrical conductivity of polymer-based nanocomposites, as expressed below [150,151]:

$$\frac{c_0(1-n_e)}{n_e+(1/3)(1-n_e)}+\frac{c_1}{3}\left[\frac{2(n_1-n_e)}{n_e+(n_1-n_e)S_{11}}+\frac{n_3-n_e}{n_e+(n_3-n_e)S_{33}}\right]=0 \tag{4}$$

where c signifies the volume fraction, subscripts 0 and 1 denote the constituent phases, and n is the conductivity ratio of each constituent phases (e.g., $n_e=\sigma_e/\sigma_0$ and $n_3=\sigma_3/\sigma_0$; σ signifies the electrical conductivity). In order to more accurately simulate the characteristics of the cementitious composites, it is necessary to include not only the air voids in cement, but also the effect of CNT waviness. Recent studies have illustrated these effects by applying multi-level homogenization method as follows [101]:

$$\frac{3(1-\phi_{CNT})(\sigma_{matrix}-\sigma_e)}{\sigma_{matrix}+2\sigma_e}+\frac{\phi_{CNT}}{3}\left[\frac{2\{(\sigma_{CNT})_{11}-\sigma_e\}}{\sigma_e+\{(\sigma_{CNT})_{11}+(\sigma_{CNT})_{33}\}S_{11}}+\frac{2\{(\sigma_{CNT})_{33}-\sigma_e\}}{\sigma_e+\{(\sigma_{CNT})_{33}-\sigma_e\}S_{33}}\right]=0 \tag{5}$$

in which

$$\sigma_{matrix}=\sigma_{cement}+\frac{\phi_{void}\sigma_{cement}\left(3-\frac{9\sigma_{cement}}{2\sigma_{cement}+\sigma_{void}}\right)}{1-\phi_{void}\left\{1+\sigma_{cement}\left(3-\frac{9\sigma_{cement}}{2\sigma_{cement}+\sigma_{void}}\right)/(\sigma_{cement}-\sigma_{void})\right\}} \tag{6}$$

with [150,151]:

$$S_{11}=S_{22}=\frac{\alpha_{wave}}{2[\alpha_{wave}{}^2-\alpha_{wave}]^{\frac{3}{2}}}\left[\alpha_{wave}(\alpha_{wave}{}^2-1)^{\frac{1}{2}}-\cosh^{-1}\alpha_{wave}\right]S_{33}=1-2S_{11} \tag{7}$$

and

$$\alpha_{wave}=\frac{4\pi L}{\{2L+DL(\theta)\}\tan\theta} \tag{8}$$

where the waviness-dependent filler length (L) can be found in [101] and the formula is utilized to predict the effective electrical conductivity of CNT-incorporated cementitious composites. Fig. 2 shows the upper and lower bounds of the electrical conductivity of CNT-incorporated cementitious composites predicted by the continuum model and compares with that experimentally obtained data

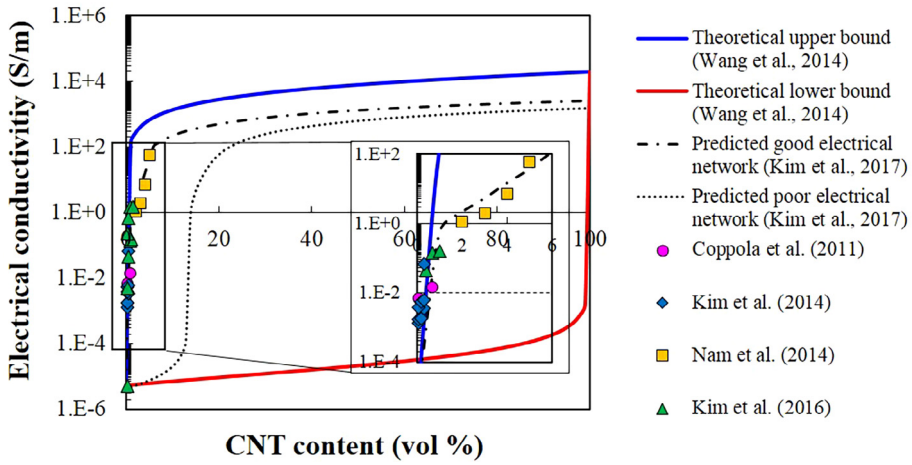

Fig. 2. Comparison of upper-lower bounds of electrical conductivity predicted by continuum model and that of cementitious composites with CNT obtained in previous studies [11,14,21,96,97].

[16,19,26,100,101]. In addition, recent numerical simulations for the analysis of CNT-incorporated cementitious nanocomposites is included in Fig. 2.

In addition, recent studies have adopted various numerical computations for the analysis of the material characteristics of CNT-incorporated cementitious nanocomposites. Yazdanbakhsh and Grasley [139] has proposed a computational methodology to calculate and quantify the theoretical maximum dispersion of nanoscale inclusions in cement paste. In particular, the w/b ratio, CNT/cement ratio and cement fineness are considered as the model parameters, indicating that the influence of geometry clustering on the dispersion of CNT particles is significant when the cement particles are agglomerated within the paste [139]. An extended finite element method (XFEM) has also proposed to investigate the mechanical and fracture characteristics of CNT/concrete specimen [152]. Based on the XFEM predictions, it is expected that the CNT can play an important role to increase the fracture energies and to delay the crack propagation [152]. However, the experimental comparisons were left to the future study, thus additional study should be followed to validate the theoretical and simulation results obtained thus far [152].

6. Application of CNT-incorporated cementitious composites

6.1. CNT-reinforced cementitious composite

The mechanical properties of CNT-incorporated cementitious composites are determined by the dispersion of CNT particles and the bonding between CNT particles and hydrates [90]. CNT particles in a poor dispersion state are agglomerated in a cementitious composite, and absorb a considerable amount of water, which evaporates later, leaving pores in the composite [16]. In addition, CNT agglomerates act as crack initiators, thereby reducing the mechanical properties of CNT-incorporated cementitious composites [90,94].

Even though a good CNT dispersion state is reached in cementitious composites, the mechanical properties of the composites can vary depending on the dispersion technique adopted. This is due to the fact that the bond strength between CNT and the cementitious composites is closely related to the dispersion technique. Cwirzen et al. [153] reported that the use of polyacrylic acid polymer as a surfactant can enhance the dispersion of CNT in cementitious composites, while it may adversely affect the bond strength between CNT and hydrates [153]. As a consequence, the compressive strength of the composites is similar to that of pure cement pastes [153]. Similar results were evidenced in other studies, which reported that such surfactants fully covered the surface of CNT and inhibited the bonding between the CNT and hydration products [17,85,95,111]. Meanwhile, the effect of surfactants on the bond strength can vary depending on the type of surfactant used. For instance, Luo et al. [95] examined the effect of the surfactant consisting of SDBS and TX10 mixed at a 3:1 ratio, and reported that the compressive and flexural strength of the CNT-incorporated composites were improved by 20.8% and 29.10%, respectively [95]. Similarly, the use of Pluronic F-127 surfactant enhanced the flexural modulus, flexural and compressive strength by 72%, 7% and 19%, respectively [97].

Surface treatment of CNT with acid was deemed to be most successful in enhancing the mechanical properties of CNT-incorporated cementitious composites [96,109–112]. This is attributed to the functional groups on the surface of CNT chemically interacting with cement hydrates, enhancing the bond strength between the CNT and the cementitious composites. Li et al. [96] conducted FT-IR analysis, and reported the chemical interaction between carboxylic acid group of acid-treated CNT and hydration products such as C-S-H and $Ca(OH)_2$ [96]. This effectively enhanced the bonding between the CNT and the hydrates in cementitious composites; under this condition, the transfer of stress was significantly improved. Consequently, cementitious composites incorporating acid-treated CNT possess enhanced flexural and compressive strength, and failure strain [96,110,112].

Meanwhile, the formation of carboxylated carbonaceous fragments (CCFs) may be triggered by acid treatment of CNT [111]. When CCFs interacts with hydrates, the incorporation of acid-treated CNT into cementitious composites does not contribute to enhancing the mechanical properties [111]; that is, CCFs inhibit the interaction between hydrates and functional groups. The adverse effect of CCFs was addressed in a study conducted by [111], in which CCFs were removed from acid-treated CNT using acetone, and the compressive strength of composites incorporating such CNT was enhanced by 60% [111].

Ultrasonication used for dispersion can also affect the mechanical properties of CNT-incorporated cementitious composites. In particular, ultrasonication treatment over an extended time can result in reducing the length of CNT, inhibiting CNT to bind neighboring C-S-H and to bridge voids [92]. Konsta-Gdoutos et al. [85] investigated the effect of length of CNT on the mechanical properties of composites using CNT with short (10–30 nm) and long (10–100 nm) length, and reported that the reinforcement level of composites incorporating 0.025–0.048 wt% of long CNT were similar to that incorporating 0.08 wt% of short CNT [85].

In other studies, the effect of incorporation of pozzolanic materials with few hundreds nanometers on the bond strength was investigated. Silica fume (10–500 nm) as a dispersion agent of CNT in cementitious composites infiltrated into CNT agglomerates, and later on formed a field of hydration, thereby acting as an anchorage between CNT and hydrates [90]. In a study by [154], nano metakaolin (NMK) was added to CNT-incorporated cementitious composites, and was effective to disrupt the attractive force among CNT particles, thereby enhancing the dispersion of CNT [154]. This effect is similar with incorporation of silica fume, in which pozzolanic materials with particle size smaller than cement particles by a factor of at least 1000 infiltrate into CNT agglomerates [154].

The amount of CNT added to cementitious composites is also an important factor in terms of mechanical properties. Fig. 3 shows the relationship between compressive strength of cementitious composites with CNT and the content of CNT [81,92,95,97,110–112,154–156]. In general, a percolation threshold, after which the electrical conductivity of CNT-incorporated cementitious composites is significantly improved, is accepted to lie between 0.3 and 0.6 wt% [16,90,157]. In contrast, the optimal amount of CNT addition in terms of mechanical properties was shown to be 0.01–0.15 wt% in Fig. 3. This amount can be correlated with a study conducted by [154], which reported the enthalpy of C-S-H in cementitious composites incorporating CNT of 0.1 wt% measured by differential scanning calorimeter is 20% lower in comparison with that in pure cement pastes [154]. That is, CNT particles wraps around cement grains, leading to a partial separation of cement grains during the hydration process. At higher dosage of CNT, this effect can reduce the bond strength by inhibiting hydration [154].

6.2. Piezoresistive sensor

Piezoresistive sensing technology refers to monitoring the electrical resistance change in a sensor, induced by an external compressive force, and evaluating the force by assessing the resistance change [158,211]. In some cases, the voltage is monitored for evaluating the externally applied force when a sensor is supplied with a constant current [118,159]. Studies of piezoresistive sensing were initiated in mid-twentieth century with development of silicon-based piezoresistive sensor, which was widely used in the field of electronic and electrical devices [160]. These studies were pioneered with introduction of new sensors with carbon-based materials incorporated in an insulating material [160]. These sensors were widely used in the field of electrical, electronic and mechanical engineering, and started to be adopted in construction and civil engineering field since late-twentieth century [160]. Specifically, these sensors can be used as a vehicle-detecting sensor for traffic, which is installed on the upper surface of road, thereby assessing the number and weight of vehicles passing the road

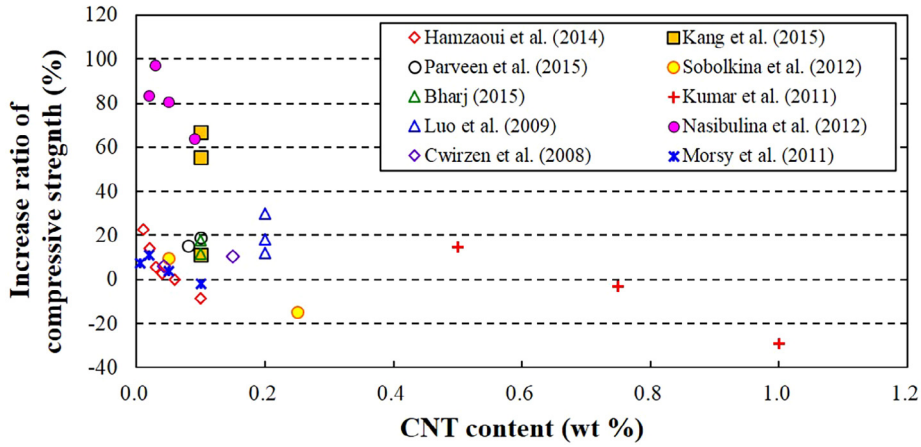

Fig. 3. Relationship between change in compressive strength (%) and CNT contents in cementitious composites [77,88,91,93,106–108,150–152].

where the sensor is installed [160].

Meanwhile, these sensors are inevitably subjected to several tons of vehicular (wheel) load, environmentally adverse effects such as significant changes in temperature and humidity, therefore, excellent mechanical properties and highly durable characteristics (especially against chemical erosion and corrosion) must be acquired [116]. This led to adoption of cement, which exhibits excellent compressive resistance against external forces, incorporating electrically conductive fillers such as metallic or carbon-based materials [160]. Among those fillers, carbon-based materials have been found to be effective for resisting against corrosion and have been assessed in numerous studies [161,162].

Carbon-based materials often incorporated in a cement-based piezoresistive sensor include carbon black, graphite, carbon fiber and carbon filament; these carbon-based materials often require modification on their surface, or use of dispersion agent such as methycellulose and silica fume [100,160]. Development of nano-sized carbon-based materials further enhanced their usage in cementitious piezoresistive sensors, owing to improved electrical conductivity and chemical stability [163]. In addition, the network of carbon nanomaterials-incorporated sensors experiences change in their electrical characteristic, exhibiting significant improvement in the sensitivity [164].

The electrical resistance change rate is a performance index of a piezoresistive sensor, and can be obtained according to the following equation.

$$\text{Electrical resistance change rate } (\%) = \frac{R_i - R_0}{R_0} \times 100 \tag{9}$$

where R_0 is the initial electrical resistance of a sensor, and also referred to as a reference value or baseline. R_i is the electrical resistance instantaneously measured. The electrical resistance change in the sensor can therefore be expressed in terms of change in R_0 relative to R_i [161]. When the externally applied force is compressive, the network in a carbon-based material becomes densified, and R_i becomes lower than that of R_0, and vice versa when the external force is tensile.

Table 1 summarizes piezoresistive characteristics of electrically conductive cementitious composites reported in previous studies [18,23,27,90,104,157,159,161,165–171]. Before the widespread of carbon nanomaterials, Wen and Chung [172] conducted a comparative study of steel fiber and carbon fiber-incorporated cementitious piezoresistive sensing composites, and reported that steel fiber incorporation showed higher electrical resistance change [165,172]. Despite the higher sensing performance observed in the steel fiber-incorporated sensor, it showed fluctuation in the electrical resistance change rate over time.

Carbon nanomaterials were utilized in later studies. Li et al. [17] adopted acid treatment and sonication of CNT for achieving sufficient degree of dispersion; CNT was first dispersed in water to which cement was added to fabricate CNT-incorporated cementitious composites [17]. The composites showed electrical resistance change of 1.7% upon external compressive force of 9.5 MPa [17]. This study was pioneered in later studies, in which incorporation of various carbon-based materials (i.e., CNT, carbon fiber) were considered in fabrication of cementitious piezoresistive sensors. Yu and Kwon [161] dispersed CNT in water via stirring process and the use of surfactant wrapping to fabricate a sensor, and reported that the composites exhibited electrical resistance change of 11.4% in response to compressive force of 8.6 MPa. The fabricated composite sensor was embedded in asphalt road, and its practical application was assessed [161]. In a study conducted by [23], MWNT was dispersed in water via sonication and surfactant wrapping to mix with cement and fabricate composite sensor; the electrical resistance change of the sensor in response to cyclic loading, and effect of water content in the composite on the electrical resistance change were evaluated [23]. The results showed that the water content above 6% decreased the max resistance change rate, indicating that piezoresistive characteristic can be adversely affected by the excessive amount of ions present in water [23]. Azhari and Banthia [27] compared the piezoresistive characteristics of cement-based sensor incorporating carbon fiber against the one incorporating carbon fiber and CNT [27]. Despite that these two sensors showed similar electrical resistance change rate given an identical loading condition, the latter sensor incorporating both carbon fiber and CNT showed more stable performance under a cyclic loading condition [27]. In other studies, Kim et al. [100] adopted use of silica fume for enhancing dispersion of CNT in cementitious composites as a piezoresistive sensor, which showed electrical resistance change of 24% at 8 MPa. Nam et al. [116] investigated the effect of CNT content on the piezoresistive sensing characteristics of cementitious composite sensor. The authors adopted surfactant wrapping and sonication for dispersing CNT, and reported that CNT content of 0.2 wt% was most effective in terms of electrical resistance change rate [116]. In particular, the electrical resistance change rate was 94% in response to a compressive force of 10 MPa, indicating that the CNT content and removing water content via drying in an oven were effective to significantly improve electrical resistance change rate [116].

In conclusion, initial studies of piezoresistive sensors based on cement adopted steel or carbon fiber, which can be considered electrically conductive microfibers. Recent studies have shown the potentials of carbon nanomaterials for use in piezoresistive sensors. Dispersion of carbon nanomaterials remains a key in the fabrication process; this has been achieved by adoption of acid treatment, surface wrapping, sonication and other techniques, which facilitated significantly improved electrical resistance change rate of sensors even at low content of CNT (0.1–0.2 wt%). The piezoresistive sensing characteristics of cement-based sensors incorporating CNT were viewed in various perspectives.

Table 1
Summary of piezoresistive characteristics of electrically conductive cementitious composites.

Materials	Piezoresistive characteristics (resistance change rate)	Ref.
Cement paste with 0.36 vol% steel fiber (8 μm diameter)	32% under loading of 6 MPa	[161]
Cement paste with 0.5 vol% carbon fiber (15 μm diameter)	2.5% under loading of 1.8 MPa	[168]
Cement paste with 2.0 wt% carbon nanofiber (20–80 nm diameter)	1.7% under loading of 5.6 MPa	[156]
Cement paste with 0.5 wt% MWNT first dispersed in water by acid treatment and sonication	12.3% under loading of 9.5 MPa	[162]
Cement paste with 0.1 wt% MWNT first dispersed in water by surfactant wrapping and stirring	11.4% under loading of 8.6 MPa	[158]
Cement paste with 0.1 wt% MWNT first dispersed in water by surfactant wrapping and sonication	5% under loading of 6 MPa	[18]
Cement mortar with 15% carbon fiber and 1% MWNT dispersed by superplasticizer incorporation and sonication	29% under loading of 10.2 MPa	[22]
Cement mortar with 0.5 vol% MWNT dispersed by incorporation of silica fume	24% under loading of 8 MPa	[86]
Cement paste with 0.1 wt% MWNT dispersed by surfactant wrapping and sonication	4.6% under loading of 4 MPa	[13]
Cement paste with 0.2 wt% MWNT dispersed in the composite by surfactant wrapping and sonication	94% under loading of 10 MPa	[100]
Cement paste with 2.0 wt% MWNT dispersed by mechanical mixing and sonication	3% under loading of 2.5 MPa	[163]
Cement paste with 0.05 wt% MWNT dispersed by surfactant wrapping and sonication	5.1% under loading of 14 MPa	[164]
Cement mortar with 0.4 wt% MWNT dispersed by magnetic stirring and sonication	17% under loading of 8 MPa	[165]
Cement paste with 1.0 wt% MWNT dispersed by surfactant wrapping and sonication	0.5% under loading of 0.64 MPa	[166]
Concrete with 0.5 wt% MWNT dispersed by surfactant wrapping and sonication	0.02% under loading of 0.8 MPa	[167]

In particular, water content was found to significantly affect their piezoresistive characteristics, implying that removal of water content in the sensor can result in dramatic improvement in the sensing capability.

6.3. Electromagnetic wave shielding material

Electromagnetic (EM) wave shielding refers to various means of reflecting the incidence of EM wave using electrically conductive materials. The principal mechanism involves reflection of EM wave to the direction of penetration or transmission, and absorption by which the wave is dissipated as heat within shielding materials [157,173]. The demand for EM wave shielding initially arose in the field of electronic devices which may be susceptible to damage, leading to a loss of integrity, reliability and compatibility due to electromagnetic interference (EMI) [174]. Nowadays, the use of electronic devices in daily life, industry, military of our society is frequent, the significance of EM wave shielding has become greater [174].

Metallic materials have been frequently used as a shielding material, due to their reflection/shielding effectiveness even at a low thickness [175]. However, their use in facilities which require a reduction in the unwanted reflection of EM wave is shown to be inadequate [175]. In addition, metallic materials are prone to degradation by humidity and chemicals, which raise concerns over their use as a shielding material [175]. This have necessitated adoption of carbon-based materials incorporated in cementitious shielding materials, which has relatively low unwanted reflection and high resistance against corrosion and chemicals [77,104]. The carbon-based materials have been used as an electrical conductive filler to enhance electrical conductivity of cementitious shielding materials, thereby serving a similar role as metallic materials. Typical materials used for this purpose include carbon fiber, graphite and carbon nanofiber. In early 2000s, CNT received attention as a new EM shielding material, attributed to its high aspect ratio which allows it to exhibit electrical current density and electrical conductivity far higher than other existing carbon-based materials [163].

EM wave shielding effectiveness (SE) is a function of EM wave reflection (SE_R), EM absorption (SE_A) and EM wave multiple reflection (SE_{MR}), as expressed in the following equation [176],

$$EM\ \ wave\ \ SE\ \ (\mathrm{dB}) = SE_R + SE_A + SE_{MR} \tag{10}$$

On the other hand, EM wave SE can also be expressed in terms of the incident EM wave energy (P_i) relative to the received energy (P_t) through a material, as expressed in the following equation [176].

$$EM\ \ wave\ \ SE = 10log\frac{P_i}{P_t} \tag{11}$$

SE_R is the quantified reflection characteristic of EM wave at the incident surface of the EM wave shielding material, while SE_A deals with the absorption characteristics attributed to the loss of EM wave via conductive loss, dielectric loss and magnetic loss [176]. Moreover, SE_R and SE_A of an EM wave shielding material can be expressed in terms of electrical conductivity σ and permeability μ as follows [176].

$$SE_R = 39.5 + 10log\frac{\sigma}{2\pi f\mu} SE_A = 8.7d\sqrt{\pi f\mu\sigma} \tag{12}$$

where f is frequency, μ is magnetic permeability and is equivalent to $\mu_0\mu_r$, in which μ_0 is $4\pi \times 10^{-7}$ H m^{-1} and μ_r is relative magnetic permeability, and σ is an electrical conductivity in terms of Ω^{-1} m^{-1}. SE_{MR}, multiple reflection of electromagnetic wave, refers to the reflection performance of an EM wave shielding material, which occurs at the opposite side of incidence of EM wave. It is often negligible, since it is much less than SE_R and SE_A. The equations above suggest that an increase in the electrical conductivity of shielding materials inevitably increases its capacity for EM wave reflection and absorption. Moreover, the reflection of EM wave is reduced by increase of EM wave frequency or permeability, while absorption is in an inverse relationship, showing an increase by increase of EM wave frequency or permeability.

Table 2 shows the shielding performance of cement-based shielding materials with various fillers, thicknesses at a given range of EM wave frequency [34,104,114,173–182]. A steel fiber is often adopted for fabrication of shielding materials, and its incorporation was reported to achieve high shielding performance (55 dB) at a relatively low content of fibers (0.9 vol%) [177]. Meanwhile, an increase in the steel fiber content was shown to be ineffective to increase its shielding performance, as evidenced by [183].

Carbon-based materials were also frequently used as a filler in cementitious shielding materials. Its implication for EM wave shielding is addressed in [178], which showed that 4.0 wt% of carbon fiber incorporated in cementitious shielding materials resulted in a shielding capacity of 21 dB at a frequency of 1 GHz. Despite that this value corresponds to a lower capacity than that of a steel fiber-incorporated cementitious shielding material, its high resistance against corrosion, chemical erosion and low unwanted reflection are highly advantageous for use as a filler in shielding materials. Other carbon-based materials used as a filler in shielding materials include carbon filament which showed 40 dB at 1 GHz, attributed to its high aspect ratio (up to 1000) [184]. Use of graphite powder and colloidal graphite in cementitious shielding materials were also reported to be successful to obtain sufficient degree of shielding capacity [182,185].

Adoption of CNT as a filler in cementitious shielding materials began in 2010. Early studies, however, reported significantly low shielding capacity of these materials (1 dB at 1 GHz), owing to deficiency in dispersion technique and low integrity of fabricated samples [34]. Later studies, in which advanced techniques of dispersion and use of admixtures were adopted, showed dramatic improvement in the shielding performance [104]. In particular, the use of 2.0 wt% CNT in a

Table 2
Shielding performance of cement-based shielding materials with various fillers, thicknesses at a given range of EM wave frequency.

Materials and sample thickness	Thickness (mm)	SE & frequency range	Ref.
Cement paste with 0.9 vol% steel fiber	4.5	55 dB (1 GHz)	[173]
Concrete with steel fiber	31.0	Absorbing 9.8 dB (2–18 GHz)	[177]
Cement mortar with 3 vol% steel fiber	5.0	37–44 dB (8–12.5 GHz)	[179]
Cement mortar with 4 wt% carbon fiber	3.9	21.1 dB (1 GHz) 18.6 dB (1.5 GHz)	[174]
Cement paste sample with 1.5 vol% carbon filament	4.0	40 dB (1 GHz)	[180]
Aluminate cement with 30 vol% graphite	3.0	10–40 dB (0.2–1.6 GHz)	[178]
Cement with 0.92 vol% colloidal graphite	4.4	22.3 dB (1 GHz) 25.6 dB (1.5 GHz)	[181]
Cement with 0.3 wt% carbon nanotube	4.5	1 dB (1 GHz) 1.5 dB (1.5 GHz)	[29]
Mortar with 0.9 wt% carbon nanotube	25.0	28 dB (2.9 GHz)	[19]
Cement with 15 wt% carbon nanotube	6.0	27 dB (12.4 GHz)	[146]
Mortar composite incorporating 2.0 wt% CNT	107.0	19 dB (1 GHz)	[182]
Cement/fly ash matrix materials with 0.6 wt% carbon nanotube	10.0	8 dB (1 GHz) 57.1 dB (18 GHz)	[100]
Cement with 3 wt% carbon nanotube of 3 wt%	30.0	9.5 dB (1 GHz)	[176]

shielding material resulted in a shielding capacity of 19 dB at 1 GHz [186]. Moreover, incorporation of fly ash was found to further increase the shielding capacity, as evidenced by [104], which showed that fly ash-incorporated CNT shielding material exhibited a shielding capacity of 8–57.1 dB at 1–18 GHz, despite its low thickness (10 mm).

In conclusion, early studies of cement-based EM wave shielding materials adopted use of steel fiber, carbon fiber and graphite, which are readily available, while adoption of CNT is recently growing. These studies include fabrication of CNT-incorporated shielding materials, and evaluating their shielding performance. Moreover, recent advances in dispersion of CNT via use of dispersion technique and admixtures showed synergistic effect, displaying few tens dB of shielding performance over a wide range of frequency at a relatively low content of CNT (1.0 wt%) [104].

6.4. Heating material

Heating can be useful and essential for civil structures in view of deicing, healthy living, hazard mitigation and industrial processing [187]. Traditional heating systems for concrete structures include ground source heat pipe, infrared heat lamps, heated fluids and solar energy. However, these inevitably accompany complicated construction, high cost, and low integrity with original structure, and therefore their application is limited [188]. Utilization of electrically conductive cementitious composites as heating material was pioneered in a study by Yehia et al. [189], and many studies were prolonged thereafter [187]. The cementitious heating materials have high structural integrity with original structures. That is, the thermal expansion-induced damage during heating is negligible, since its thermal expansion coefficient is similar with that of the original cementitious structures [187].

Heating of electrically conductive cementitious composites occurs via Joule-heating mechanism, in which heat is generated by a current flowing through a conductor [190,191]. The heat generation capability of electrically conductive cementitious composites is highly associated with its resistance, as expressed by the Joule's first law [192]:

$$Q = \frac{V^2}{R} \times t \tag{13}$$

In this equation, Q (J) denotes the heat generated, V represents the electrical voltage applied to the conductor with resistance (R) during time (t) [192]. The heat generated in Eq. (11) is proportional to the square of electrical voltage, while the heat generation capacity is inversely proportional to the resistance; that is, the heat generation capability of electrically conductive cementitious composites can be enhanced by lowering the resistivity of the composites, referring to Ohm's law [16]. Another factor governing the heat generation capacity of electrically conductive cementitious composites is a power density [193], as expressed below [194].

$$\text{Power density } (\text{W/m}^2) = IP/(Pe \times D) \tag{14}$$

here, IP (watt) is the input power applied to the electrically conductive cementitious composites and is computed by a product of the input voltage and current, Pe is the perimeter (m) around which an electrode and the electrically conductive cementitious composites are in contact, and D is the distance (m) between the two electrodes. Accordingly, electrically conductive cementitious composites with a higher power density is inevitably inherited with higher heat generation capacity [193]. Thus, low resistivity and high power density are desirable properties for electrically conductive cementitious composites to be used for heating.

Before the introduction of CNT for incorporation in a cementitious heating composite, use of various types of fillers, such as steel fiber, steel shaving, carbon fiber, carbon black and graphite, were attempted. The use of these conventional fillers for fabrication of electrically conductive cementitious composites, however, faced technical limitations, i.e., the resistivity of a steel fiber-incorporated electrically conductive cementitious composites significantly increases over time. This is due to a layer of passive film formed around steel fiber in the alkaline environment of cementitious materials [195]. This effect can be amount to an increase in the resistivity 60 times higher after one year, and can be a factor which significantly degrades the heating performance of cementitious composites [193]. Similarly, the content of graphite in cementitious composites has to exceed 15.0 wt%, while the excessive dosage of graphite can significantly reduce the mechanical properties of the composites. For instance, the compressive strength of cementitious composites incorporating a graphite of 20.0 wt% was as low as 2 MPa in previous study [196].

Recently, many studies were conducted to evaluate the heat generation capacity of cementitious composites incorporating CNT. Kim et al. [16] explored the heat generation capacity of cementitious composites incorporating a CNT of 0.1–2.0 wt% under monotonic and cyclic heating condition, and reported that the heat generation capacity and heat-induced mechanical properties of cementitious composites was stable when the content of CNT was 0.6 wt% [16]. Kim et al. conducted a further study to improve the heating performance and stability of cementitious composites with CNT [197]. In that study, carbon fiber was used to form a hierarchically conductive pathways in cementitious composites with CNT and reported that the heating performance and stability of the composite with CNT and carbon fiber were clearly improved, compared to that of cementitious composites with CNT [197,210]. The improvement of the heating performance and stability was possibly caused by the overlapped areas between carbon fiber and

Table 3
Summary of heating performance of electrically conductive cementitious composites.

Filler type	Filler content (wt%)	Electrical resistivity (Ω·cm)	Temperature increase (°C)	Heating rate (°C/hr)	Input voltage (V)	Power density (W/m^2)	Δρ*	Reference
Graphite	17.3	0.8×10^5-1.5×10^5	35	7	220	660	0.38 × 10^5–0.5 × 10^5	[117]
Steel fiber/carbon fiber/graphite	7.8/0.7/4.0	320	21.8	10.9	44	1500–4000	–	[189]
Steel fiber	140	500–1000	32	8.4	35	520	600	[185]
Steel fiber/Graphite	11.7/50	101–395	47	102.6	140	3000–6000	350	[195]
Graphite	5.0	> 2.5 × 10^5	33.2	19.52	150	931	2.49 × 10^5	[196]
Carbon fiber	5.0	> 2.5 × 10^5	42.3	24.9	150	1095	2.49 × 10^5	
Steel fiber	4.0	0.85	41.6	50.7	7.1	750	–	[173]
CNT	0.6	145.2	34.6	2.41	8	4494	9	[194]

* Δρ: reduction in the electrical resistivity of electrically conductive cementitious composites induced by negative temperature coefficient effect.

CNT [197]. The overlapped areas mitigated the damage of electrically conductive pathways during heating [197].

Table 3 summarizes electrical and heating characteristics of electrically conductive cementitious composites reported in previous studies [16,121,189,192,193,198–200]. In most case, the electrical resistivity of cementitious composites with conventional conductive fillers was more than 300 Ω•cm and the input voltage applied to the composites was more than 30 V [121,189,193,198,199]. Moreover, the reduction in the electrical resistivity of cementitious composites was relatively significant, compared to that of the composites with a resistivity of lower than 100 Ω•cm [16,121,199]. The reduction in the electrical resistivity of cementitious composites during heating, which is called negative temperature coefficient (NTC) effect, is caused by tunneling effect [16]. Tunneling effect is induced by the thermally activated electron [24]. The thermally activated electrons can hop the insulation gaps, leading to the voltage fluctuation and a decrease in the resistivity [24,201]. The tunneling effect occurs at a distance equal to or less than 10 nm [202]. The current density between two conductive fillers can be expressed as the following equation, according to tunneling theory equation of Simmons [24]

$$\mathrm{PJ} = \left[\frac{3(2m\varphi)^{\frac{1}{2}}}{2s}\right](e/h)^2 U \bullet exp\left[-\left(\frac{4\pi s}{h}\right)(2m\varphi)^{1/2}\right] \quad (15)$$

where, m, e and h are the electron mass, charge on an electron and Planck's constant, respectively. φ, s and U are the height of tunnel potential barrier, potential barrier width and voltage applied across barrier [24]. According to the equation, tunneling current is exponential with barrier width, meaning that the resistivity of electrically conductive cementitious composites is reduced as the distance between conductive fillers decreases [24]. The thermal expansion of cementitious composites during heating induces the fillers to be straighter and closer, leading to a decrease in the distance between the fillers and a reduction in its resistivity [202]. Thus, the relatively high voltage applied to cementitious composites with high electrical resistivity can exhibit significant reduction in the resistivity of the composites during heating and thereby cause a rapid increase in heating rate and thermal shock [199]. This not only degrades the structural integrity of the heating composite, but can also cause fatal damage in a human body [199].

The electrical resistivity of cementitious composites with CNT is relatively low, compared to cementitious composites with conventional conductive fillers, and the content of CNT added to cementitious composites to ensure the low electrical resistivity was lower than 0.6 wt % [16,197]. Furthermore, the power density of cementitious composites with a CNT of 0.6 wt% was approximately 4494 W/m^2, while the content of conventional conductive fillers was more than 7.0 wt% to ensure the power density similar to that of the composites with CNT. It can be inferred from the facts that the incorporation of CNT in cementitious composites is favorable to ensure the heating performance and stability. Nevertheless, studies on heating stability and durability of the composites are only few and additional work is necessary.

7. Recent research advances

Recent studies of CNT-incorporated cementitious composites include the synthesis of CNT-incorporated heterogeneous materials to improve mechanical properties and functionalities of the composites. Kim et al. [203] reported development of covalently-synthesized CNT and silica fume which increased the compressive modulus of calcium silicate hydrates, and hence, improved the mechanical properties of the cementitious composites. The compressive strength of the composites incorporating the synthesis was approximately two times higher than that of the cement pastes [203]. It was attributable that the pozzolanic materials such as silica fume synthesized with CNT acted as an anchor and improved the load transfer from hydrates to CNT particles [203]. In another work by Zhang et al. [204], electrostatic self-assembled CNT and nano-carbon black (CNT/NCB) was used as an electrically conductive filler, and the use of electrostatic self-assembled CNT/NCB improved the piezoresistive properties of the cementitious composites. The stress sensitivity of the composites with CNT/NCB fillers was approximately two times higher than that of the cementitious composites incorporating CNT only [204]. Meanwhile, CNT-incorporated cementitious composites have shown their viability in medical applications. Pahlevanzadeh et al. [205] synthesized methyl methacrylate (PPMA) bone cement incorporating monticellite (Mon) and CNT, and reported that the incorporation of CNT in PPMA-Mon improved the mechanical properties due to the crack resistance inherited by the CNT [205]. Furthermore, favorable bioactivity of PPMA-Mon was improved by the incorporation of CNT, since the incorporation of CNT in the bone cement promoted the attachment of MG63 cell [205].

Durability aspects of cementitious composites incorporating CNT is a topic of increasing number of studies in recent years. Hawreen and Bogas [206] investigated the creep and shrinkage characteristics of cementitious composites incorporating CNT. It was reported in the previous study that the incorporation of CNT in cementitious composites reduced the long-time dependent shrinkage and the creep up to approximately 15% and 18%, respectively [206]. It was also observed that the high aspect ratio of CNT is more favorable for reducing the shrinkage of the cementitious composites [206]. Kim et al. [207] reported that the incorporation of CNT reduced the autogenous shrinkage of the cementitious composites more than 10%, since the CNT particles added to the composites inhibited the hydration of cement particles at an early age of curing and bridged among the hydrates.

A number of recent studies include the use of cementitious binders other than Portland cement, i.e., alkali-activated cement and geopolymer [213–215]. However, the pore chemistry with high alkalinity due to the use of alkali activators such as NaOH, and the rheological characteristics significantly differ from those observed in Portland cement-based composites. In particular, the use of superplasticizers typically used to disperse CNT in Portland cement-based composites is found ineffective due to the high alkalinity which leads to instability of

the superplasticizers [208]. Therefore, the application of existing dispersion techniques excluding the use of the superplasticizers have been attempted in the fabrication of geopolymer incorporating CNT. Da Luz Graziele et al. [209] utilized pristine and carboxyl-functionalized CNT to fabricate metakaolin-based geopolymer by employing ultrasonication to disperse the CNT particles. This study also reported that the ultrasonication method was not effective when the pristine CNT content was 0.2% by the weight of the binder [209]. In contrast, the functionalized CNT particles were effectively dispersed in the geopolymer pastes through ultrasonication process [209].

Overall, recent studies on the cementitious composites incorporating CNT are focused on the synthesis of CNT-incorporated heterogeneous materials to improve the mechanical properties and functionalities, the application of CNT to alternative cementitious systems, and the durability of the composites. However, further studies are necessary to explore the long-term functionalities of the cementitious composites incorporating CNT, in relation to the durability.

8. Conclusions

The present paper provides information on the structure and extraordinary properties of CNT, analyzes the mechanism of various dispersion techniques of CNT applied to the cementitious composites, and introduces the evaluation and prediction methods for the dispersion state of CNT in cementitious composites. Furthermore, the studies on the applicability of cementitious composites incorporating CNT in terms of reinforcement, electromagnetic shielding, piezoresistive sensing and heating are summarized to provide valuable information which can result in a further studies on improvement of those research areas. The following concluding remarks are drawn from the present study.

(1) Carbon nanotube has remarkable mechanical, electrical, thermal properties and chemical stability induced by its unique structural characteristics. In order to improve the various properties of cementitious composites through the incorporation of CNT, the proper dispersion of CNT should be ensured for the fabrication of CNT-incorporated cementitious composites. The understanding of physio-mechanical/chemical dispersion mechanism of CNT in cementitious composites is certainly helpful for material design of CNT-incorporated functional cementitious composites.
(2) Various dispersion techniques such as ultrasonication, use of admixtures, siliceous materials, minimization of w/b ratio, modification of CNT have been attempted to disperse CNT particles in cementitious composites. However, most of techniques have pros and cons. The pros and cons of each dispersion techniques summarized in the present study may contribute to the development of new dispersion techniques of CNT in cementitious composites.
(3) Dispersion state of CNT in cementitious composites was evaluated experimentally and theoretically. Experimental techniques for the evaluation of dispersion state of CNT can be broadly divided into image-based (SEM, AFM, optical microscope and so on) and resistivity measurement analysis.
(4) Theoretically, micromechanics-based models for 3D randomly oriented CNT-reinforced cement composites are introduced. The considerations of inherent voids and CNT waviness in the cementitious composites are incorporated into the micromechanics-based model for a more precise prediction. Various experimental data and numerical simulations are included to illustrate the influence of morphological characteristic of CNT on the electrical characteristic of cement composites.
(5) Potential applicability and the theoretical backgrounds of functional cementitious composites incorporating CNT were introduced in the present study. The proper CNT contents to improve the mechanical properties of cementitious composites was in the range of 0.01–0.15% by the weight of cement. The improvement of electrical properties of cementitious composites resulting from the incorporation of CNT facilitated the use of the composites as piezoresistive sensor, electromagnetic wave shielding material, and heating composites. The piezoresistive, electromagnetic wave shielding and heating performances of CNT-incorporated cementitious composites were compared to those of the cementitious composites with conventional electrically conductive fillers. The use of this promising nanomaterials improved the various functional properties of the CNT-incorporated cementitious composites compared to those of cementitious composites incorporating conventional conductive fillers.
(6) The incorporation of CNT into cementitious composites contributed to overcoming the functional limitations of the composites utilizing conventional conductive fillers. However, further studies should be conducted to investigate functional stability and durability of the composites based on the understanding cement chemistry.

Acknowledgements

This research was supported by the National Research Foundation (NRF) of South Korea with a grant (2018R1A2A1A05076894) funded by the Ministry of Science and ICT (MSIT), and by the National Strategic Project-Carbon Upcycling of the NRF funded by the MSIT, the Ministry of Environment (ME) and the Ministry of Trade, Industry and Energy (MOTIE) (2017M3D8A2084752).

References

[1] Iijima S. Helical microtubules of graphitic carbon. Nature 1991;354:56.
[2] Salvetat J-P, Bonard J-M, Thomson N, Kulik A, Forro L, Benoit W, et al. Mechanical properties of carbon nanotubes. Appl Phys A 1999;69:255–60.
[3] Saito R, Dresselhaus G, Dresselhaus MS. Physical properties of carbon nanotubes. World Scientific; 1998.
[4] Zhang Q, Chen G, Yoon S, Ahn J, Wang S, Zhou Q, et al. Thermal conductivity of multiwalled carbon nanotubes. Int J Thermal Sci 2002;66:165440.
[5] Bal S, Samal SS. Carbon nanotube reinforced polymer composites—a state of the art. Bullet Mater Sci 2007;30:379.
[6] Spitalsky Z, Tasis D, Papagelis K, Galiotis CJ. Carbon nanotube–polymer composites: chemistry, processing, mechanical and electrical properties. Prog Polymer Sci 2010;35:357–401.
[7] Inam F, Yan H, Reece M, Peijs TJ. Structural and chemical stability of multiwall carbon nanotubes in sintered ceramic nanocomposite. Adv Appl Ceram 2010;109:240–7.
[8] Curtin WA, Sheldon BW. CNT-reinforced ceramics and metals. Mater Today 2004;7:44–9.
[9] Liu C, Fan Y, Liu M, Cong H, Cheng H, Dresselhaus MS. Hydrogen storage in single-walled carbon nanotubes at room temperature. Science 1999;286:1127–9.
[10] De Heer WA, Chatelain A, Ugarte D. A carbon nanotube field-emission electron source. Science 1995;270:1179–80.
[11] Nguyen L, Phi T, Phan P, Vu H, Nguyen-Duc C, Fossard F. Synthesis of multi-walled carbon nanotubes for NH3 gas detection. Physica E 2007;37:54–7.
[12] Jia Z, Wang Z, Xu C, Liang J, Wei B, Wu D, et al. Study on poly (methyl methacrylate)/carbon nanotube composites. Mater Sci Eng, A 1999;271:395–400.
[13] Huang H, Liu C, Wu Y, Fan S. Aligned carbon nanotube composite films for thermal management. Adv Mater 2005;17:1652–6.
[14] Yu S, Zheng W, Yu W, Zhang Y, Jiang Q, Zhao Z. Formation mechanism of β-phase in PVDF/CNT composite prepared by the sonication method. Macromolecules 2009;42:8870–4.
[15] Lee H, Kim H, Cho MS, Choi J, Lee Y. Fabrication of polypyrrole (PPy)/carbon nanotube (CNT) composite electrode on ceramic fabric for supercapacitor applications. Electrochim Acta 2011;56:7460–6.
[16] Kim GM, Naeem F, Kim HK, Lee HK. Heating and heat-dependent mechanical characteristics of CNT-embedded cementitious composites. Compos Struct 2016;136:162–70.
[17] Li GY, Wang PM, Zhao X. Pressure-sensitive properties and microstructure of carbon nanotube reinforced cement composites. Cem Concr Compos 2007;29:377–82.
[18] Konsta-Gdoutos MS, Aza CA. Self sensing carbon nanotube (CNT) and nanofiber (CNF) cementitious composites for real time damage assessment in smart structures. Cem Concr Compos 2014;53:162–9.
[19] Coppola L, Buoso A, Corazza F. Electrical properties of carbon nanotubes cement composites for monitoring stress conditions in concrete structures. Appl Mech Mater: Trans Tech Publ 2011:118–23.
[20] Han B, Yu X, Kwon E, Ou J. Effects of CNT concentration level and water/cement ratio on the piezoresistivity of CNT/cement composites. J Compos Mater 2012;46:19–25.
[21] Sharma S, Kothiyal N. Synergistic effect of zero-dimensional spherical carbon

nanoparticles and one-dimensional carbon nanotubes on properties of cement-based ceramic matrix: microstructural perspectives and crystallization investigations. Compos Interfaces 2015;22:899–921.
[22] D'Alessandro A, Rallini M, Ubertini F, Materazzi AL, Kenny JM. Investigations on scalable fabrication procedures for self-sensing carbon nanotube cement-matrix composites for SHM applications. Cem Concr Compos 2016;65:200–13.
[23] Han B, Yu X, Ou J. Effect of water content on the piezoresistivity of MWNT/cement composites. J Mater Sci 2010;45:3714–9.
[24] Wang G, Xiao H, Li H, Guan X. A scouring sensor by using the electrical properties of carbon nanotube-filled cement-based composite. Sensors and Smart Structures Technologies for Civil, Mechanical and Aerospace Systems 2013. International Society for Optics and Photonics; 2013. p. 869239.
[25] Aza CA, Danoglidis PA, Konsta-Gdoutos MS. Self sensing capability of multifunctional cementitious nanocomposites. Nanotechnology in construction. Springer; 2015. p. 363–9.
[26] Nam I. Electromagnetic wave shielding/absorbing characteristics of CNT embedded cement composites PhD Thesis Korea: Advanced Institute of Science and Technology (KAIST); 2014
[27] Azhari F, Banthia N. Cement-based sensors with carbon fibers and carbon nanotubes for piezoresistive sensing. Cem Concr Compos 2012;34:866–73.
[28] Cha S, Song C, Cho Y, Choi S. Piezoresistive properties of CNT reinforced cementitious composites. Mater Res Innov 2014;18. S2-716-S2-21.
[29] Jin L, Bower C, Zhou O. Alignment of carbon nanotubes in a polymer matrix by mechanical stretching. Appl Phys Lett 1998;73:1197–9.
[30] Shaffer MS, Windle AH. Fabrication and characterization of carbon nanotube/poly (vinyl alcohol) composites. Adv Mater 1999;11:937–41.
[31] Needleman A, Borders T, Brinson L, Flores V, Schadler L. Effect of an interphase region on debonding of a CNT reinforced polymer composite. Compos Sci Technol 2010;70:2207–15.
[32] Ramasubramaniam R, Chen J, Liu H. Homogeneous carbon nanotube/polymer composites for electrical applications. Appl Phys Lett 2003;83:2928–30.
[33] Glenn J. Nanotechnology in concrete: state of the art and practice. Chem Phys Lett 2004;392:242–8.
[34] Nam I-W, Kim H-K, Lee H-K. Influence of silica fume additions on electromagnetic interference shielding effectiveness of multi-walled carbon nanotube/cement composites. Constr Build Mater 2012;30:480–7.
[35] Manzur T, Yazdani N. Strength enhancement of cement mortar with carbon nanotubes: early results and potential. Transp Res Record: J Transp Res Board 2010:102–8.
[36] Han B, Ding S, Yu X. Intrinsic self-sensing concrete and structures: a review. Measurement 2015;59:110–28.
[37] Reales OAM, Toledo Filho RD. A review on the chemical, mechanical and microstructural characterization of carbon nanotubes-cement based composites. Constr Build Mater 2017;154:697–710.
[38] Mendes T, Hotza D, Repette W. Nanoparticles in cement based materials: a review. Rev Adv Master Sci. 2015;40:89–96.
[39] Bastos G, Patino-Barbeito F, Patino-Cambeiro F, Armesto J. Nano-inclusions applied in cement-matrix composites: a review. Materials 2016;9:1015.
[40] Dong W, Li W, Tao Z, Wang K. Piezoresistive properties of cement-based sensors: review and perspective. Constr Build Mater 2019;203:146–63.
[41] Shi T, Li Z, Guo J, Gong H, Gu C. Research progress on CNTs/CNFs-modified cement-based composites–a review. Constr Build Mater 2019;202:290–307.
[42] Tang W, Santare MH, Advani SG. Melt processing and mechanical property characterization of multi-walled carbon nanotube/high density polyethylene (MWNT/HDPE) composite films. Carbon 2003;41:2779–85.
[43] Terrones M. Science and technology of the twenty-first century: synthesis, properties, and applications of carbon nanotubes. Annu Rev Mater Res 2003;33:419–501.
[44] Okada S, Saito S, Oshiyama A. Energetics and electronic structures of encapsulated C 60 in a carbon nanotube. Phys Rev Lett 2001;86:3835.
[45] Yamabe T, Fukui K, Tanaka K. The science and technology of carbon nanotubes. Elsevier; 1999.
[46] Maiti A. Carbon nanotubes: Bandgap engineering with strain. Nat Mater 2003;2:440.
[47] Kelly BT. Physics of graphite; 1981.
[48] Kelly A, Macmillan NH. Strong solids. Walton Street, Oxford OX 2 6 DP, UK: Oxford University Press; 1986.
[49] Overney G, Zhong W, Tomanek D. Structural rigidity and low frequency vibrational modes of long carbon tubules. Z Phys D Atoms, Mol Clusters 1993;27:93–6.
[50] Treacy MJ, Ebbesen T, Gibson J. Exceptionally high Young's modulus observed for individual carbon nanotubes. Nature 1996;381:678.
[51] Wong EW, Sheehan PE, Lieber CM. Nanobeam mechanics: elasticity, strength, and toughness of nanorods and nanotubes. Science 1997;277:1971–5.
[52] Falvo MR, Clary G, Taylor Ii R, Chi V, Brooks Jr F, Washburn S, et al. Bending and buckling of carbon nanotubes under large strain. Nature 1997;389:582.
[53] Endo M, Takeuchi K, Kobori K, Takahashi K, Kroto HW, Sarkar A. Pyrolytic carbon nanotubes from vapor-grown carbon fibers. Carbon 1995;33:873–81.
[54] Shibutani Y, Shiozaki M, Kugimiya T, Tomita Y. Irreversible deformation of carbon nanotubes under bending. Nippon Kinzoku Gakkaishi 1999;63:1262–8.
[55] Yu M-F, Files BS, Arepalli S, Ruoff RS. Tensile loading of ropes of single wall carbon nanotubes and their mechanical properties. Phys Rev Lett 2000;84:5552.
[56] Wang Z, Gao R, Poncharal P, De Heer W, Dai Z, Pan Z. Mechanical and electrostatic properties of carbon nanotubes and nanowires. Mater Sci Eng, C 2001;16:3–10.
[57] Ren Z, Huang Z, Xu J, Wang J, Bush P, Siegal M, et al. Synthesis of large arrays of well-aligned carbon nanotubes on glass. Science 1998;282:1105–7.
[58] Tans SJ, Verschueren AR, Dekker C. Room-temperature transistor based on a single carbon nanotube. Nature 1998;393:49.
[59] Wei B, Vajtai R, Ajayan P. Reliability and current carrying capacity of carbon nanotubes. Appl Phys Lett 2001;79:1172–4.
[60] Langer L, Stockman L, Heremans J, Bayot V, Olk C, Van Haesendonck C, et al. Electrical resistance of a carbon nanotube bundle. J Mater Res 1994;9:927–32.
[61] Dai H, Wong EW, Lieber CM. Probing electrical transport in nanomaterials: conductivity of individual carbon nanotubes. Science 1996;272:523–6.
[62] Ebbesen T, Lezec H, Hiura H, Bennett J, Ghaemi H, Thio T. Electrical conductivity of individual carbon nanotubes. Nature 1996;382:54.
[63] Ruoff RS, Lorents DC. Mechanical and thermal properties of carbon nanotubes. Carbon 1995;33:925–30.
[64] Hone J. Phonons and thermal properties of carbon nanotubes. Carbon nanotubes. Springer; 2001. p. 273–86.
[65] Maultzsch J, Reich S, Thomsen C, Dobardžić E, Milošević I, Damnjanović M. Phonon dispersion of carbon nanotubes. Solid State Commun 2002;121:471–4.
[66] Ishii H, Kobayashi N, Hirose K. Electron–phonon coupling effect on quantum transport in carbon nanotubes using time-dependent wave-packet approach. Physica E 2007;40:249–52.
[67] Maeda T, Horie C. Phonon modes in single-wall nanotubes with a small diameter. Physica B 1999;263:479–81.
[68] Kasuya A, Saito Y, Sasaki Y, Fukushima M, Maedaa T, Horie C, et al. Size dependent characteristics of single wall carbon nanotubes. Mater Sci Eng, A 1996;217:46–7.
[69] Popov V. Theoretical evidence for T1/2 specific heat behavior in carbon nanotube systems. Carbon 2004;42:991–5.
[70] Stroscio MA, Dutta M, Kahn D, Kim KW. Continuum model of optical phonons in a nanotube. Superlattices Microstruct 2001;29:405–9.
[71] Grujicic M, Cao G, Gersten B. Atomic-scale computations of the lattice contribution to thermal conductivity of single-walled carbon nanotubes. Mater Sci Eng, B 2004;107:204–16.
[72] Hepplestone S, Ciavarella A, Janke C, Srivastava G. Size and temperature dependence of the specific heat capacity of carbon nanotubes. Surf Sci 2006;600:3633–6.
[73] Yu C, Shi L, Yao Z, Li D, Majumdar A. Thermal conductance and thermopower of an individual single-wall carbon nanotube. Nano Lett 2005;5:1842–6.
[74] Kim P, Shi L, Majumdar A, McEuen PL. Thermal transport measurements of individual multiwalled nanotubes. Phys Rev Lett 2001;87:215502.
[75] Thostenson ET, Ren Z, Chou T-W. Advances in the science and technology of carbon nanotubes and their composites: a review. Compos Sci Technol 2001;61:1899–912.
[76] Sanchez F, Sobolev K. Nanotechnology in concrete–a review. Constr Build Mater 2010;24:2060–71.
[77] Ajayan PM, Schadler LS, Braun PV. Nanocomposite science and technology. John Wiley & Sons; 2006.
[78] Lourie O, Cox D, Wagner H. Buckling and collapse of embedded carbon nanotubes. Phys Rev Lett 1998;81:1638.
[79] Thess A, Lee R, Nikolaev P, Dai H, Petit P, Robert J, et al. Crystalline ropes of metallic carbon nanotubes. Science 1996;273:483–7.
[80] Girifalco L, Hodak M, Lee RS. Carbon nanotubes, buckyballs, ropes, and a universal graphitic potential. Phys Rev B 2000;62:13104.
[81] Bharj J. Experimental study on compressive strength of cement-CNT composite paste. Indian J Pure Appl Phys (IJPAP). 2015;52:35–8.
[82] Vaisman L, Wagner HD, Marom G. The role of surfactants in dispersion of carbon nanotubes. Adv Colloid Interface Sci 2006;128:37–46.
[83] Yu J, Grossiord N, Koning CE, Loos J. Controlling the dispersion of multi-wall carbon nanotubes in aqueous surfactant solution. Carbon 2007;45:618–23.
[84] Hielscher T. Ultrasonic production of nano-size dispersions and emulsions. arXiv preprint arXiv:07081831; 2007.
[85] Konsta-Gdoutos MS, Metaxa ZS, Shah SP. Multi-scale mechanical and fracture characteristics and early-age strain capacity of high performance carbon nanotube/cement nanocomposites. Cem Concr Compos 2010;32:110–5.
[86] Ma P-C, Siddiqui NA, Marom G, Kim J-K. Dispersion and functionalization of carbon nanotubes for polymer-based nanocomposites: a review. Compos A Appl Sci Manuf 2010;41:1345–67.
[87] Makar J, Beaudoin J. Carbon nanotubes and their application in the construction industry. Special Publication-Royal Society of Chemistry; 2004. p. 331–42. 292.
[88] Lu K, Lago R, Chen Y, Green M, Harris P, Tsang S. Mechanical damage of carbon nanotubes by ultrasound. Carbon 1996;34:814–6.
[89] Mukhopadhyay K, Dwivedi CD, Mathur GN. Conversion of carbon nanotubes to carbon nanofibers by sonication. Carbon 2002;8:1373–6.
[90] Kim H, Nam IW, Lee H-K. Enhanced effect of carbon nanotube on mechanical and electrical properties of cement composites by incorporation of silica fume. Compos Struct 2014;107:60–9.
[91] Rastogi R, Kaushal R, Tripathi S, Sharma AL, Kaur I, Bharadwaj LM. Comparative study of carbon nanotube dispersion using surfactants. J Colloid Interface Sci 2008;328:421–8.
[92] Sobolkina A, Mechtcherine V, Khavrus V, Maier D, Mende M, Ritschel M, et al. Dispersion of carbon nanotubes and its influence on the mechanical properties of the cement matrix. Cem Concr Compos 2012;34:1104–13.
[93] Yazdanbakhsh A, Grasley Z, Tyson B, Al-Rub RA. Carbon nano filaments in cementitious materials: some issues on dispersion and interfacial bond. Special Publication; 2009. p. 21–34. 267.
[94] Collins F, Lambert J, Duan WH. The influences of admixtures on the dispersion, workability, and strength of carbon nanotube–OPC paste mixtures. Cem Concr Compos 2012;34:201–7.
[95] Luo J, Duan Z, Li H. The influence of surfactants on the processing of multi-walled

carbon nanotubes in reinforced cement matrix composites. Physica Status Solidi (a) 2009;206:2783–90.
[96] Li GY, Wang PM, Zhao X. Mechanical behavior and microstructure of cement composites incorporating surface-treated multi-walled carbon nanotubes. Carbon 2005;43:1239–45.
[97] Parveen S, Rana S, Fangueiro R, Paiva MC. Microstructure and mechanical properties of carbon nanotube reinforced cementitious composites developed using a novel dispersion technique. Cem Concr Res 2015;73:215–27.
[98] Wen S, Chung D. Carbon fiber-reinforced cement as a strain-sensing coating. Cem Concr Res 2001;31:665–7.
[99] Fu X, Chung D. Self-monitoring of fatigue damage in carbon fiber reinforced cement. Cem Concr Res 1996;26:15–20.
[100] Kim H, Park I, Lee H-K. Improved piezoresistive sensitivity and stability of CNT/cement mortar composites with low water–binder ratio. Compos Struct 2014;116:713–9.
[101] Kim G, Yang B, Cho K, Kim E, Lee H-K. Influences of CNT dispersion and pore characteristics on the electrical performance of cementitious composites. Compos Struct 2017;164:32–42.
[102] Chen X, Wu S. Influence of water-to-cement ratio and curing period on pore structure of cement mortar. Constr Build Mater 2013;38:804–12.
[103] Nochaiya T, Chaipanich A. Behavior of multi-walled carbon nanotubes on the porosity and microstructure of cement-based materials. Appl Surf Sci 2011;257:1941–5.
[104] Nam IW, Lee H-K. Synergistic effect of MWNT/fly ash incorporation on the EMI shielding/absorbing characteristics of cementitious materials. Constr Build Mater 2016;115:651–61.
[105] Szleifer I, Yerushalmi-Rozen R. Polymers and carbon nanotubes—dimensionality, interactions and nanotechnology. Polymer 2005;46:7803–18.
[106] O'Connell MJ, Boul P, Ericson LM, Huffman C, Wang Y, Haroz E, et al. Reversible water-solubilization of single-walled carbon nanotubes by polymer wrapping. Chem Phys Lett 2001;342:265–71.
[107] Bandyopadhyaya R, Nativ-Roth E, Regev O, Yerushalmi-Rozen R. Stabilization of individual carbon nanotubes in aqueous solutions. Nano Lett 2002;2:25–8.
[108] Cui J, Wang W, You Y, Liu C, Wang P. Functionalization of multiwalled carbon nanotubes by reversible addition fragmentation chain-transfer polymerization. Polymer 2004;45:8717–21.
[109] Musso S, Tulliani J-M, Ferro G, Tagliaferro A. Influence of carbon nanotubes structure on the mechanical behavior of cement composites. Compos Sci Technol 2009;69:1985–90.
[110] Cwirzen A, Habermehl-Cwirzen K, Penttala V. Surface decoration of carbon nanotubes and mechanical properties of cement/carbon nanotube composites. Adv Cem Res 2008;20:65–73.
[111] Nasibulina LI, Anoshkin IV, Nasibulin AG, Cwirzen A, Penttala V, Kauppinen EI. Effect of carbon nanotube aqueous dispersion quality on mechanical properties of cement composite. J Nanomater 2012;2012:35.
[112] Kang S-T, Seo J-Y, Park S-H. The characteristics of CNT/cement composites with acid-treated MWCNTs. Adv Mater Sci Eng 2015;2015.
[113] Sanchez F, Ince C. Microstructure and macroscopic properties of hybrid carbon nanofiber/silica fume cement composites. Compos Sci Technol 2009;69:1310–8.
[114] Singh AP, Gupta BK, Mishra M, Chandra A, Mathur R, Dhawan S. Multiwalled carbon nanotube/cement composites with exceptional electromagnetic interference shielding properties. Carbon 2013;56:86–96.
[115] Nam IW, Lee H. Image analysis and DC conductivity measurement for the evaluation of carbon nanotube distribution in cement matrix. Int J Concr Struct Mater 2015;9:427–38.
[116] Nam I, Souri H, Lee H-K. Percolation threshold and piezoresistive response of multi-wall carbon nanotube/cement composites. Smart Struct Syst 2015.
[117] Wansom S, Kidner N, Woo L, Mason T. AC-impedance response of multi-walled carbon nanotube/cement composites. Cem Concr Compos 2006;28:509–19.
[118] Han B, Guan X, Ou J. Electrode design, measuring method and data acquisition system of carbon fiber cement paste piezoresistive sensors. Sens Actuators, A 2007;135:360–9.
[119] Han S, Yan P, Kong X. Study on the compatibility of cement-superplasticizer system based on the amount of free solution. Sci China Technol Sci 2011;54:183–9.
[120] Cao J, Chung D. Electric polarization and depolarization in cement-based materials, studied by apparent electrical resistance measurement. Cem Concr Res 2004;34:481–5.
[121] Wu T, Huang R, Chi M, Weng T. A study on electrical and thermal properties of conductive concrete. Comp Concr 2013;12:337–49.
[122] Haga K, Shibata M, Hironaga M, Tanaka S, Nagasaki S. Change in pore structure and composition of hardened cement paste during the process of dissolution. Cem Concr Res 2005;35:943–50.
[123] Whittington H, McCarter J, Forde M. The conduction of electricity through concrete. Mag Concr Res 1981;33:48–60.
[124] Chacko RM, Banthia N, Mufti AA. Carbon-fiber-reinforced cement-based sensors. Can J Civ Eng 2007;34:284–90.
[125] Xie P, Gu P, Beaudoin JJ. Electrical percolation phenomena in cement composites containing conductive fibres. J Mater Sci 1996;31:4093–7.
[126] Garboczi EJ, Bentz DP, Frohnsdorff G. The past, present, and future of the computational materials science of concrete. Proceedings of the J Francis young symposium (materials science of concrete workshop). Citeseer; 2000.
[127] Faucon P, Delaye J, Virlet J, Jacquinot J, Adenot F. Study of the structural properties of the C· S· H (I) BY molecular dynamics simulation. Cem Concr Res 1997;27:1581–90.
[128] Churakov SV. Hydrogen bond connectivity in jennite from ab initio simulations. Cem Concr Res 2008;38:1359–64.
[129] Abdolhosseini Qomi MJ, Ulm FJ, Pellenq RJM. Evidence on the dual nature of aluminum in the calcium-silicate-hydrates based on atomistic simulations. J Am Ceram Soc 2012;95:1128–37.
[130] Korb J-P, McDonald P, Monteilhet L, Kalinichev A, Kirkpatrick R. Comparison of proton field-cycling relaxometry and molecular dynamics simulations for proton–water surface dynamics in cement-based materials. Cem Concr Res 2007;37:348–50.
[131] Pellenq RJ-M, Kushima A, Shahsavari R, Van Vliet KJ, Buehler MJ, Yip S, et al. A realistic molecular model of cement hydrates. Proc Natl Acad Sci 2009;106:16102–7.
[132] Manzano H, Durgun E, Abdolhosseine Qomi MJ, Ulm F-J, Pellenq RJ, Grossman JC. Impact of chemical impurities on the crystalline cement clinker phases determined by atomistic simulations. Cryst Growth Des 2011;11:2964–72.
[133] Ji Q, Pellenq RJ-M, Van Vliet KJ. Comparison of computational water models for simulation of calcium–silicate–hydrate. Comput Mater Sci 2012;53:234–40.
[134] Pellenq RJ-M, Van Damme H. Why does concrete set?: the nature of cohesion forces in hardened cement-based materials. Mrs Bulletin 2004;29:319–23.
[135] Gmira A, Zabat M, Pellenq R-M, Van Damme H. Microscopic physical basis of the poromechanical behavior of cement-based materials. Mater Struct 2004;37:3–14.
[136] Masoero E, Del Gado E, Pellenq R-M, Ulm F-J, Yip S. Nanostructure and nanomechanics of cement: polydisperse colloidal packing. Phys Rev Lett 2012;109:155503.
[137] Masoero E, Del Gado E, Pellenq RJ-M, Yip S, Ulm F-J. Nano-scale mechanics of colloidal C-S–H gels. Soft Matter 2014;10:491–9.
[138] Ioannidou K, Pellenq RJ-M, Del Gado E. Controlling local packing and growth in calcium–silicate–hydrate gels. Soft Matter 2014;10:1121–33.
[139] Yazdanbakhsh A, Grasley Z. The theoretical maximum achievable dispersion of nanoinclusions in cement paste. Cem Concr Res 2012;42:798–804.
[140] Klein ML, Shinoda W. Large-scale molecular dynamics simulations of self-assembling systems. Science 2008;321:798–800.
[141] Allen AJ, Thomas JJ, Jennings HM. Composition and density of nanoscale calcium–silicate–hydrate in cement. Nat Mater 2007;6:311.
[142] Ishida T, Kishi T, Maekawa K. Multi-scale modeling of structural concrete. CRC Press; 2014.
[143] Unger JF, Eckardt S. Multiscale modeling of concrete. Arch Comput Methods Eng 2011;18:341.
[144] Konsta-Gdoutos MS, Metaxa ZS, Shah SP. Highly dispersed carbon nanotube reinforced cement based materials. Cem Concr Res 2010;40:1052–9.
[145] Herakovich CT. Mechanics of fibrous composites; 1998.
[146] Yang B, Shin H, Lee H-K, Kim H. A combined molecular dynamics/micromechanics/finite element approach for multiscale constitutive modeling of nanocomposites with interface effects. Appl Phys Lett 2013;103:241903.
[147] Eshelby JD. The determination of the elastic field of an ellipsoidal inclusion, and related problems. Proc R Soc Lond A 1957;241:376–96.
[148] Eshelby JD. The elastic field outside an ellipsoidal inclusion. Proc R Soc Lond A 1959;252:561–9.
[149] Yang B, Shin H, Kim H, Lee H-K. Strain rate and adhesive energy dependent viscoplastic damage modeling for nanoparticulate composites: Molecular dynamics and micromechanical simulations. Appl Phys Lett 2014;104:101901.
[150] Weng GJ. A dynamical theory for the Mori-Tanaka and Ponte Castañeda-Willis estimates. Mech Mater 2010;42:886–93.
[151] Wang Y, Weng GJ, Meguid SA, Hamouda AM. A continuum model with a percolation threshold and tunneling-assisted interfacial conductivity for carbon nanotube-based nanocomposites. J Appl Phys 2014;115:193706.
[152] Eftekhari M, Ardakani SH, Mohammadi S. An XFEM multiscale approach for fracture analysis of carbon nanotube reinforced concrete. Theor Appl Fract Mech 2014;72:64–75.
[153] Cwirzen A, Habermehl-Cwirzen K, Nasibulin A, Kaupinen E, Mudimela P, Penttala V. SEM/AFM studies of cementitious binder modified by MWCNT and nano-sized Fe needles. Mater Charact 2009;60:735–40.
[154] Morsy M, Alsayed S, Aqel M. Hybrid effect of carbon nanotube and nano-clay on physico-mechanical properties of cement mortar. Constr Build Mater 2011;25:145–9.
[155] Kumar S, Kolay P, Malla S, Mishra S. Effect of multiwalled carbon nanotubes on mechanical strength of cement paste. J Mater Civ Eng 2011;24:84–91.
[156] Hamzaoui R, Guessasma S, Mecheri B, Eshtiaghi AM, Bennabi A. Microstructure and mechanical performance of modified mortar using hemp fibres and carbon nanotubes. Mater Des 2014;56(1980–2015):60–8.
[157] Nam I, Lee H-K, Jang J. Electromagnetic interference shielding/absorbing characteristics of CNT-embedded epoxy composites. Compos A Appl Sci Manuf 2011;42:1110–8.
[158] Kang I, Schulz MJ, Kim JH, Shanov V, Shi D. A carbon nanotube strain sensor for structural health monitoring. Smart Mater Struct 2006;15:737.
[159] Galao O, Baeza FJ, Zornoza E, Garcés P. Strain and damage sensing properties on multifunctional cement composites with CNF admixture. Cem Concr Compos 2014;46:90–8.
[160] Mosser V, Suski J, Goss J, Obermeier E. Piezoresistive pressure sensors based on polycrystalline silicon. Sens Actuators, A 1991;28:113–32.
[161] Yu X, Kwon E. A carbon nanotube/cement composite with piezoresistive properties. Smart Mater Struct 2009;18:055010.
[162] Banthia N, Bindiganavile V, Jones J, Novak J. Fiber-reinforced concrete in precast concrete applications: research leads to innovative products. PCI J 2012;57.
[163] Hong S, Myung S. Nanotube electronics: a flexible approach to mobility. Nat Nanotechnol 2007;2:207.
[164] Hu N, Karube Y, Yan C, Masuda Z, Fukunaga H. Tunneling effect in a polymer/

carbon nanotube nanocomposite strain sensor. Acta Mater 2008;56:2929–36.
[165] Wen S, Chung D. A comparative study of steel-and carbon-fibre cement as piezoresistive strain sensors. Adv Cem Res 2003;15:119–28.
[166] Li H, Xiao H-G, Ou J-P. A study on mechanical and pressure-sensitive properties of cement mortar with nanophase materials. Cem Concr Res 2004;34:435–8.
[167] García-Macías E, Downey A, D'Alessandro A, Castro-Triguero R, Laflamme S, Ubertini F. Enhanced lumped circuit model for smart nanocomposite cement-based sensors under dynamic compressive loading conditions. Sens Actuators, A 2017;260:45–57.
[168] Sasmal S, Ravivarman N, Sindu B, Vignesh K. Electrical conductivity and piezoresistive characteristics of CNT and CNF incorporated cementitious nanocomposites under static and dynamic loading. Compos A Appl Sci Manuf 2017;100:227–43.
[169] Jeevanagoudar YV, Krishna RH, Gowda R, Preetham R, Prabhakara R. Improved mechanical properties and piezoresistive sensitivity evaluation of MWCNTs reinforced cement mortars. Constr Build Mater 2017;144:188–94.
[170] Downey A, D'Alessandro A, Ubertini F, Laflamme S, Geiger R. Biphasic DC measurement approach for enhanced measurement stability and multi-channel sampling of self-sensing multi-functional structural materials doped with carbon-based additives. Smart Mater Struct 2017;26:065008.
[171] Meoni A, D'Alessandro A, Downey A, García-Macías E, Rallini M, Materazzi AL, et al. An experimental study on static and dynamic strain sensitivity of embeddable smart concrete sensors doped with carbon nanotubes for SHM of large structures. Sensors 2018;18:831.
[172] Wen S, Chung D. Uniaxial compression in carbon fiber-reinforced cement, sensed by electrical resistivity measurement in longitudinal and transverse directions. Cem Concr Res 2001;31:297–301.
[173] Chung D. Electromagnetic interference shielding effectiveness of carbon materials. Carbon 2001;39:279–85.
[174] Kim H-G, Lee H-K. Development of electromagnetic wave absorbing/shielding construction materials. Magazine of the Korea Concrete Institute; 2008. p. 20.
[175] Kim B, Lee H-K, Kim E, Lee S-H. Intrinsic electromagnetic radiation shielding/absorbing characteristics of polyaniline-coated transparent thin films. Synth Met 2010;160:1838–42.
[176] Al-Saleh MH, Sundararaj U. Electromagnetic interference shielding mechanisms of CNT/polymer composites. Carbon 2009;47:1738–46.
[177] Wen S, Chung D. Electromagnetic interference shielding reaching 70 dB in steel fiber cement. Cem Concr Res 2004;34:329–32.
[178] Chiou J-M, Zheng Q, Chung D. Electromagnetic interference shielding by carbon fibre reinforced cement. Composites 1989;20:379–81.
[179] Wang B, Guo Z, Han Y, Zhang T. Electromagnetic wave absorbing properties of multi-walled carbon nanotube/cement composites. Constr Build Mater 2013;46:98–103.
[180] Micheli D, Vricella A, Pastore R, Delfini A, Morles RB, Marchetti M, et al. Electromagnetic properties of carbon nanotube reinforced concrete composites for frequency selective shielding structures. Constr Build Mater 2017;131:267–77.
[181] Yang H-Y, Li J, Ye Q-Z. Research on absorbing EMW properties of steel-fiber concrete. J Funct Mater 2002;33:341–3.
[182] Yue Z, Rentao Z, Fengwu Z, Jimei X, Runzhang Y, Shixi O. Electromagnetic interference shielding effectiveness of graphite-MDF cement composite. Chinese J Mater Res 1995;9:284–8.
[183] Kwon S, Lee H-K. A computational approach to investigate electromagnetic shielding effectiveness of steel fiber-reinforced mortar. Computers, Mater Continua (CMC) 2009;12:197.
[184] Fu X, Chung D. Submicron-diameter-carbon-filament cement-matrix composites. Carbon 1998;36:459–62.
[185] Cao J, Chung D. Colloidal graphite as an admixture in cement and as a coating on cement for electromagnetic interference shielding. Cem Concr Res 2003;33:1737–40.
[186] Micheli D, Pastore R, Vricella A, Morles RB, Marchetti M, Delfini A, et al. Electromagnetic characterization and shielding effectiveness of concrete composite reinforced with carbon nanotubes in the mobile phones frequency band. Mater Sci Eng, B 2014;188:119–29.
[187] Chung D. Self-heating structural materials. Smart Mater Struct 2004;13:562.
[188] Zhang K, Han B, Yu X. Nickel particle based electrical resistance heating cementitious composites. Cold Reg Sci Technol 2011;69:64–9.
[189] Yehia S, Tuan CY. Conductive concrete overlay for bridge deck deicing. Materials J 1999;96:382–90.
[190] Liu Q, Schlangen E, García Á, van de Ven M. Induction heating of electrically conductive porous asphalt concrete. Constr Build Mater 2010;24:1207–13.
[191] Ding Y, Chen Z, Han Z, Zhang Y, Pacheco-Torgal F. Nano-carbon black and carbon fiber as conductive materials for the diagnosing of the damage of concrete beam. Constr Build Mater 2013;43:233–41.
[192] Wang S, Wen S, Chung D. Resistance heating using electrically conductive cements. Adv Cem Res 2004;16:161–6.
[193] Wu J, Liu J, Yang F. Three-phase composite conductive concrete for pavement deicing. Constr Build Mater 2015;75:129–35.
[194] Alleman J, Althani H, Noufi R, Moutinho H, Al-Jassim M, Hasoon F. Dependence of the characteristics of Mo films on sputter conditions. Golden, CO (United States): National Renewable Energy Lab. (NREL); 2000.
[195] Li H, Zhang Q, Xiao H. Self-deicing road system with a CNFP high-efficiency thermal source and MWCNT/cement-based high-thermal conductive composites. Cold Reg Sci Technol 2013;86:22–35.
[196] Qin Z, Wang Y, Mao X, Xie X. Development of graphite electrically conductive concrete and application in grounding engineering. New Build Mater. 2009;11:46–8.
[197] Kim G, Yang B, Yoon H, Lee H-K. Synergistic effects of carbon nanotube and carbon fiber on heat generation and electrical characteristics of cementitious composites. Carbon 2018;134:283–92.
[198] Kim G, Yang B, Ryu G, Lee H-K. The electrically conductive carbon nanotube (CNT)/cement composites for accelerated curing and thermal cracking reduction. Compos Struct 2016;158:20–9.
[199] Tuan CY, Yehia S. Evaluation of electrically conductive concrete containing carbon products for deicing. Materials J 2004;101:287–93.
[200] Gomis J, Galao O, Gomis V, Zornoza E, Garcés P. Self-heating and deicing conductive cement. Experimental study and modeling. Constr Build Mater 2015;75:442–9.
[201] Sheng P. Fluctuation-induced tunneling conduction in disordered materials. Phys Rev B 1980;21:2180.
[202] Xiang ZD, Chen T, Li ZM, Bian XC. Negative temperature coefficient of resistivity in lightweight conductive carbon nanotube/polymer composites. Macromol Mater Eng 2009;294:91–5.
[203] Kim G, Kim Y, Kim Y, Seo J, Yang B, Lee H-K. Enhancement of the modulus of compression of calcium silicate hydrates via covalent synthesis of CNT and silica fume. Constr Build Mater 2019;198:218–25.
[204] Zhang L, Ding S, Li L, Dong S, Wang D, Yu X, et al. Effect of characteristics of assembly unit of CNT/NCB composite fillers on properties of smart cement-based materials. Compos A Appl Sci Manuf 2018;109:303–20.
[205] Pahlevanzadeh F, Bakhsheshi-Rad H, Ismail A, Aziz M, Chen X. Development of PMMA-Mon-CNT bone cement with superior mechanical properties and favorable biological properties for use in bone-defect treatment. Mater Lett 2019;240:9–12.
[206] Hawreen A, Bogas J. Creep, shrinkage and mechanical properties of concrete reinforced with different types of carbon nanotubes. Constr Build Mater 2019;198:70–81.
[207] Kim G, Yoon H, Lee H-K. Autogenous shrinkage and electrical characteristics of cement pastes and mortars with carbon nanotube and carbon fiber. Constr Build Mater 2018;177:428–35.
[208] Salami BA, Johari MAM, Ahmad ZA, Maslehuddin M. Impact of added water and superplasticizer on early compressive strength of selected mixtures of palm oil fuel ash-based engineered geopolymer composites. Constr Build Mater 2016;109:198–206.
[209] da Luz G, Gleize PJP, Batiston ER, Pelisser F. Effect of pristine and functionalized carbon nanotubes on microstructural, rheological, and mechanical behaviors of metakaolin-based geopolymer. Cem Concr Compos 2019.
[210] Kim GM, Park SM, Ryu GU, Lee HK. Electrical characteristics of hierarchical conductive pathways in cementitious composites incorporating CNT and carbon fiber. Cem Concr Compos 2017;82:165–75.
[211] Nam IW, Park SM, Lee HK, Zheng L. Mechanical properties and piezoresistive sensing capabilities of FRP composites incorporating CNT fibers. Compos Struct 2017;178:1–8.
[212] Kim GM, Nam IW, Yoon HN, Lee HK. Effect of superplasticizer type and siliceous materials on the dispersion of carbon nanotube in cementitious composites. Compos Struct 2018;185:264–72.
[213] Park SM, Jang JG, Lee HK. Unlocking the role of MgO in the carbonation of alkali-activated slag cement. Inorg Chem Front 2018;5(7):1661–70.
[214] Park SM, Jang JG, Chae SA, Lee HK. An NMR spectroscopic investigation of aluminosilicate gel in alkali-activated fly ash in a CO_2-rich environment. Mater 2016;9(5):308.
[215] Park SM, Jang JG, Lee NK, Lee HK. Physicochemical properties of binder gel in alkali-activated fly ash/slag exposed to high temperatures. Cem Concr Res 2016;89:72–9.